

DELPHYNE: A PRE-TRAINED MODEL FOR GENERAL AND FINANCIAL TIME SERIES

Xueying Ding

Carnegie Mellon University
xding2@cs.cmu.edu

Aakriti Mittal

Bloomberg
amittal114@bloomberg.net

Achintya Gopal

Bloomberg*
achintyagopal@gmail.com

ABSTRACT

Time-series data is a vital modality within data science communities. This is particularly valuable in financial applications, where it helps in detecting patterns, understanding market behavior, and making informed decisions based on historical data. Recent advances in language modeling have led to the rise of time-series pre-trained models that are trained on vast collections of datasets and applied to diverse tasks across financial domains. However, across financial applications, existing time-series pre-trained models have not shown boosts in performance over simple finance benchmarks in both zero-shot and fine-tuning settings. This phenomenon occurs because of a i) lack of financial data within the pre-training stage, and ii) the negative transfer effect due to inherently different time-series patterns across domains. Furthermore, time-series data is continuous, noisy, and can be collected at varying frequencies and with varying lags across different variables, making this data more challenging to model than languages. To address the above problems, we introduce a Pre-trained MoDEL for FINance TimE-series (**Delphyne**). **Delphyne** achieves competitive performance to existing foundation and full-shot models with few fine-tuning steps on publicly available datasets, and also shows superior performances on various financial tasks.

1 INTRODUCTION

Time series is one of the most ubiquitous modalities in finance. Time-series analysis is critical to various tasks, such as asset pricing, volatility modeling, risk management, economic indicator analysis, etc. Traditional statistical methods for financial time series include Autoregressive Integrated Moving Average (ARIMA), Generalized Autoregressive Conditional Heteroskedasticity (GARCH), and Vector Autoregressive (VAR) models. In recent years, deep learning-based methods are being applied to these financial tasks (e.g., Horvath et al. (2019); Araujo & Gaglione (2023); Liu et al. (2024e); Gopal (2024)).

Following the surge of large language models (LLMs), research has explored the possibility of large deep-learning models for time-series analysis. One approach focuses on prompting and adapting existing pre-trained language models for time-series tasks (Zhou et al., 2023; Jin et al., 2024; Chang et al., 2023; Gruver et al., 2023), while another line of research trains foundation models directly on time-series data (Woo et al., 2024; Das et al., 2024; Goswami et al., 2024). Both approaches aim to train a single model with large-scale cross-domain data that can be applied to various tasks, as opposed to full-shot methods that require training a distinct model for each dataset.

However, previous research indicates that directly prompting LLMs for financial tasks brings only modest benefits; moreover, most LLM-based research focuses only on forecasting directional trends of stock returns, offering fewer practical applications than traditional methods (Chen et al., 2023; Yu et al., 2023; Lopez-Lira & Tang, 2023). Preliminary experiments also reveal that pre-trained models do not demonstrate significant improvement over GARCH in risk analysis (Sec. 5).

One reason for this limitation is that the existing public datasets for pre-training lack sufficient financial data to learn patterns and distributional properties that are specific to time-series data in finance. Jointly training on financial data alongside public datasets presents an additional challenge:

*Work done while employed at Bloomberg.

the substantial differences between domains can lead to *negative transfer*. Negative transfer has been extensively discussed within the literature, defined as a case when “transferring knowledge from the training data has an negative impact on the target tasks” (Wang et al., 2019). Negative transfer is identified as a key obstacle towards pre-training graph foundation model (Wang et al., 2024a; Mao et al., 2024), yet is not explored within the context of time-series data. In Sec. H, we show that the negative transfer effect is a real challenge when pre-training time-series models. Cross-domain transfer learning is particularly difficult, as time-series data tends to be noisier and more continuous compared to languages and images. To alleviate the negative transfer effect, we believe that fine-tuning is the only remedy. We contend that the strength of pre-trained time-series models lies in their capacity to rapidly “unlearn” the biases of the pre-training stage and “adapt” to the specific distribution of new tasks, given limited training data and time.

Building on our observation and analysis of negative transfer, we introduce our pre-trained time-series model, which incorporates several architectural modifications designed to better handle time-series data and tasks. Time-series data often involve an arbitrary number of variates, each collected at different frequencies (e.g., where quarterly profit growth is forecasted from daily or weekly sales data). Additionally, finance tasks often involve nowcasting, where some variates contain contemporaneous data. Our model is an encoder-based transformer that employs the any-variante attention mechanism, introduced by Woo et al. (2024). In addition, we implement a missing data mask alongside the forecast mask, which enhances the model’s ability to adapt to cross-frequency training while minimizing negative interference (Van Ness et al., 2023).

Probabilistic forecasting is an essential feature required for uncertainty quantification and anomaly detection within time series. Existing literature either assumes a fixed output distribution (Salinas et al., 2020a) or utilizes a mixture of several distributions (Woo et al., 2024). However, when the underlying data exhibits contrasting distributions and supports, a single distribution may be inadequate. Our model simplifies the output by using a mixture of Student-T distributions, which are widely used in finance for heavy-tailed tasks. In our preliminary studies, this approach shows comparable performance to Woo et al. (2024) on downstream tasks.

In Sec. 3, we introduce additional architectural modifications and present corresponding ablation studies. To this end, we train our Pre-Trained MoDEL for FINance TimE-series (**Delphyne**), the first time-series model capable of both general and finance-specific tasks. Delphyne is trained on both LOTSA (the largest public times-series dataset (Woo et al., 2024)) and financial data (Sec.4). We conduct experiments for both general and finance time-series tasks, demonstrating that Delphyne consistently outperforms or matches state-of-the-art baselines. Our key contributions are as follows:

- Demonstrate the presence of negative transfer in pre-trained time-series models, highlighting how this effect sets them apart from LLMs, emphasizing that the value of pre-trained time-series models lies in their fine-tuning capability, which mitigates the negative transfer effect and enhances downstream performance with minimal iterations.
- Introduce several architectural modifications in our model and demonstrate their significance through comprehensive ablation studies.
- Delphyne is the first time-series pre-trained model to excel in both general time-series tasks and a variety of downstream finance tasks.

2 NEGATIVE TRANSFER EFFECT

Negative transfer has been widely studied in foundation models across different modalities (Wang et al., 2024a). This problem is typically seen as the model’s reduced performance on downstream tasks due to mismatches between the source training data and the target distribution (Wang et al., 2019). However, this phenomenon has not been thoroughly explored in the context of time series. In pre-trained time-series models, negative transfer can occur when cross-domain data is added during pre-training. The appearances of data from too different distributions can lead to less effective zero-shot forecast results, even if we feed the downstream tasks within similar domains. We present three examples to highlight the presence of negative transfer, particularly focusing on the difficulties of cross-domain transfer from finance data to other areas.

Pre-training with GARCH and Wavelet Data To simulate datasets encountered in real-world scenarios, we generate two types of synthetic data: Wavelet functions and GARCH-style data. Wavelet

functions are composed of a combination of sine and cosine waves, while in GARCH models the current time-steps are based on past squared residuals and past variances, frequently used to capture volatility clustering seen in financial time-series data. These data types are prevalent in nature and are standard simulations for time series in both finance and non-finance literature (Bollerslev, 1986; Das et al., 2024; Petrozziello et al., 2022). Fig. 1 shows examples of these two data types.

We trained three distinct models: the first on GARCH-style data (G-Model), the second on Wavelet data (W-Model), and the third on a combination of both, using half Wavelet and half GARCH data (M-Model). Each model utilizes a standard autoregressive transformer decoder without any additional embeddings or patching. Further details can be found in the Appendix H.1. Table 1 presents the negative log-likelihood (NLL) for each model’s zero-shot forecasts with context lengths of 32 and 128. As expected, the mixed-data model (M-Model), trained on both GARCH and Wavelet data, performs significantly worse in terms of zero-shot NLL compared to the models trained on a single data source. This underperformance is likely due to the differing frequencies and structures of GARCH and Wavelet data.

Bayesian MCMC While the previous example showcases that model trained on both GARCH and Wavelet data underperforms compared to models trained on a single type, one may argue that it is a model training problem. However, we provide further evidence that negative transfer occurs because of the contrasting properties of the data, regardless of the model used.

We analyze the time-series pre-trained models in a Bayesian framework, in analogy to the Bayesian inference mechanism in (Müller et al., 2022; Hollmann et al., 2023). The pre-training stage is essential to fit a good prior to the training tasks. Given N tasks (datasets) $\{\mathcal{D}_i\}_{i=1}^N$, the learned parameters $\hat{\mathbf{w}}$ implicitly presents the maximum likely distribution over all observed tasks by minimizing the pre-training objective. As shown by Müller et al. (2022), optimizing the following training loss approximates the true Bayesian posterior forecast distribution for time series:

$$\mathbb{E}_{x_{1:t+1} \sim p(D)} [-\log q_\theta(x_{t+1}|x_{1:t})] \quad (1)$$

In light of this framework, we can simulate the results of zero-shot learning by setting the prior to some data generating process (instead of learning from data). To illustrate our approach, we first construct a model to simulate the data-generating processes of Wavelet functions, and then generate corresponding observed data. We subsequently apply Markov Chain Monte Carlo (MCMC) to obtain posterior samples for the model (the distribution of model parameters after conditioning on the observed data). Note that the Wavelet model is fully aware of the underlying data-generating process, and it should be capable of modeling the distribution accurately, apart from the additive Gaussian noise. Then, we fit a mixture of Wavelets and GARCH to the same data, see Appendix H.2.

We compute the NLL and Mean Squared Error (MSE) for the fitted Wavelet-MCMC model and the Mixture-MCMC model. The results are summarized in Table 2. Despite having full knowledge of the underlying data generation processes for both the Wavelet and GARCH functions, the mixture model struggles to accurately approximate the posterior distribution in zero-shot forecasts, resulting in higher NLL and MSE compared to models trained on a single function type. This illustrates the phenomenon of negative transfer, where incorporating too many variations of data can negatively impact the modeling of the posterior distribution.

Delphyne Training We observe similar effects while training our Delphyne model. During the pre-training phase, we evaluate different checkpoints to assess the zero-shot forecast performance on the ETTh2 dataset for two versions of our model: Delphyne-A (trained with the LOTSA and financial data) and Delphyne-L (trained without financial data).

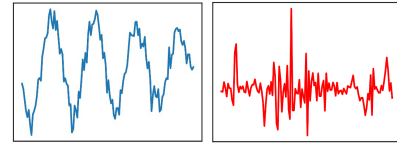


Figure 1: (Left) Wavelet Function. (Right) GARCH-style data.

Table 1: Zero-shot NLL(\downarrow) for models trained on different data types.

Model	Wavelet Pred.	GARCH Pred.
G-Model-128	-	0.0865
W-Model-128	-0.1020	-
M-Model-128	-0.0733	0.1137
G-Model-32	-	0.0882
W-Model-32	-0.1330	-
M-Model-32	-0.0732	0.1176

Table 2: Forecasted NLL(\downarrow) and MSE(\downarrow) for Wavelet-MCMC, and Mixture-MCMC model.

Model	MSE.	NLL.
Wavelet-MCMC	0.1058	0.2692
Mixture-MCMC	0.1127	0.2937

We record the average Mean Absolute Error (MAE) across forecast lengths of 96 and 196. Additionally, we evaluate the fine-tuning performance of both models using MAE as the loss objective. Initially, Delphyne-A incurs a higher MAE than Delphyne-L, but after fine-tuning, both models achieve comparable MAE. For in-distribution forecasting on Monash dataset, we also observe that Delphyne-A underperforms Delphyne-L with larger aggregated MAEs. However, both methods perform comparably after fine-tuning (Sec. 5.2).

A Framework to Relate Pre-training to Downstream Performance The three examples above demonstrate that negative transfer can indeed occur when pre-training time-series data from various domains. The continuous nature of time-series data, combined with its inherent noise and significant variability across domains, makes pre-training a model for time-series particularly challenging compared to other modalities like language and images.

Given the negative transfer phenomenon, why do we need to build a pre-trained time-series model? The strength of a pre-trained time-series model lies in its ability to quickly adapt to downstream tasks with finetuning on only a few training samples, which offers great time and data efficiency in comparison to full shot models. We aim to develop a pre-trained time-series model that can swiftly adjust to new task distributions by efficiently “unlearning” pre-training biases and “adapting” to the specific characteristics of downstream tasks, even with limited training data or minimal gradient updates. In the next section, we detail our design choices and present ablation studies that underscore the critical role of these design elements in enabling the model to rapidly and effectively adapt during the fine-tuning stage.

3 MODEL OVERVIEW

Problem Formulation For any-variate times-series, assuming that each dataset $\mathcal{D} = \{\mathbf{Y}^{(i)}\}_{i=1}^M$ has M data points, while each $\mathbf{Y}^{(i)} \in \mathbb{R}^{l(i) \times T_{\mathbf{Y}^{(i)}}}$, contains $l(i)$ ($l(i) \geq 1$) variates and $T_{\mathbf{Y}^{(i)}}$ time-steps. We formulate the pre-training as a forecasting task: for each variate j , the future $h_j \geq 0$ time-steps are forecasted by modeling their forecast distribution: $P(\mathbf{Y}_{T_{\mathbf{Y}}-\mathbf{h}:T_{\mathbf{Y}}} | \phi)$, where ϕ is the output distribution of the time-series forecasting model and \mathbf{h} is a vector comprised of h_j time-steps. The overall training objective is:

$$\min_{\mathbf{w}} \mathbb{E}_{P(\mathbf{Y}) \sim \mathcal{D}} [-\log P(\mathbf{Y}_{T_{\mathbf{Y}}-\mathbf{h}:T_{\mathbf{Y}}} | \phi)] \quad \text{s.t. } \phi \leftarrow f_{\mathbf{w}}(\mathbf{Y}_{T_{\mathbf{Y}}-p:T_{\mathbf{Y}}-\mathbf{h}}) \quad (2)$$

where we define \mathbf{h} as the forecast length and p as the look-back window length. Note that the number of time-steps conditioned on for each time series is different: $h_j - p$. We formulate our problem in this way where the number of time-steps to forecast is different per time series in order to allow for nowcasting where the information available for each time series can be different.

Time-series data, particularly in finance, exhibit unique characteristics that present distinct challenges:

1. **Multivariate Nature:** The variable \mathbf{Y} typically has a dimensionality $k > 1$, indicating the presence of multiple interrelated time series. For example, US stocks are often quite correlated with the S&P 500 index.
2. **Nowcasting Data:** The data of some variables is often available with considerable time lag, so it is important to estimate current value of the time-series based on its own recent history and current values of other variables. This is the nowcasting task in economics and financial applications.
3. **Multifrequency and Missing Data:** Each \mathbf{Y} variable can be collected at varying granularities—such as individual tick data versus aggregated bar data—or may contain numerous missing entries due to irregular sampling intervals.
4. **Extended Context Length:** Unlike natural languages, where input sequences are generally in the range of hundreds of tokens, financial time-series data often span thousands of timesteps, requiring models to handle significantly longer temporal dependencies.

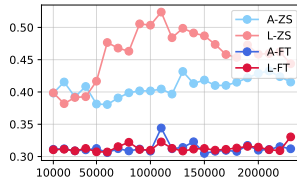


Figure 2: MAE on ETTh2 across (average forecast length of {96, 192}) training. Finance data hurts zero-shot (ZS) performance of Delphyne-A on ETTh2, but finetune (FT) eventually “undoes” the effect.

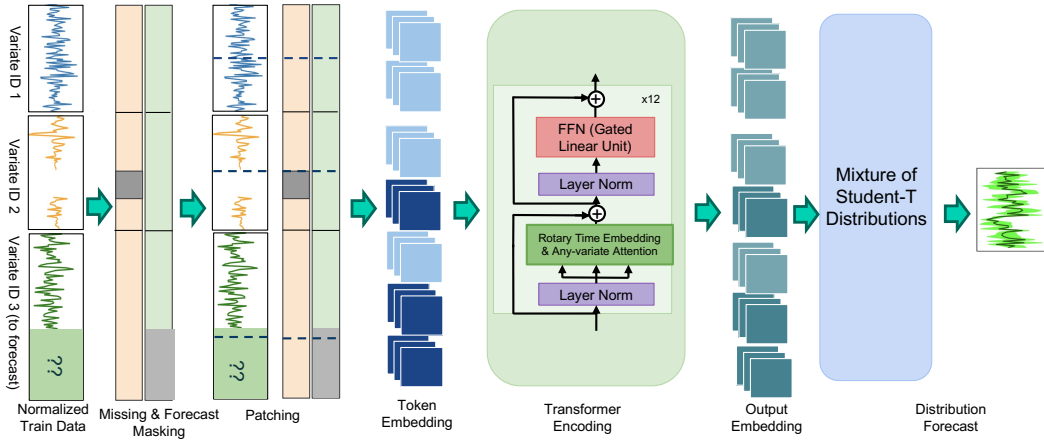


Figure 3: Delphyne Overview

3.1 OVERALL ARCHITECTURE

Following recent approaches (Woo et al., 2024; Goswami et al., 2024), we adopt a transformer encoder structure as the backbone of Delphyne. Fig. 3 shows the overall pipeline.

Padding. To handle the multivariate nature of time-series data and accommodate the flexibility of varying the number of variates and covariates, we flatten and concatenate all variates along a single dimension. Each variate is assigned a unique identifier, and instance normalization is applied independently (Kim et al., 2022). For shorter time-series data, we pad the time series on the right (after forecast mask); prior literature pads to the left Woo et al. (2024); Goswami et al. (2024), but since we want to handle time series where each can have a variable-length, we must right-pad.

Missing and Forecast Masking Before Patching. Recent work shows that patching time series allows the model to attend to significantly longer contexts (Nie et al., 2023). Therefore, Delphyne breaks the flattened time series into disjoint patches, fixing the patch size to 32. Contrary to prior work, we create a [FORECAST MASK] to identify the target timesteps for forecast as well as a [MISSING MASK] that indicates where data is unobserved due to the sampling procedure. For many finance tasks, data is collected at multiple frequencies or sampled irregularly, often leading to missing time steps (e.g., daily stock prices not being recorded on holidays). Simply ignoring these gaps can misalign multifrequency data, while backfilling or zero-filling distorts the original data distribution and can produce unsatisfactory forecast. We treat missing data similarly to forecast masks during training; however, we exclude the missing values from the forecast process. We apply both masks alongside the time-series data and learn a trainable linear projection to generate time-series embeddings that incorporate both data and missingness information. These patch embeddings serve as input to the transformer model. We suspect that applying masking before patching may lead to less effective token embeddings but is necessary for managing missingness in financial tasks.

Attention Block. The transformer encoder utilizes pre-normalization (Xiong et al., 2020), rotary positional embedding (Su et al., 2024), any-variate attention (Sec. 3.3), Silu activation function (Elfwing et al., 2018) and gated linear unit (GLU) (Shazeer, 2020) to replace FFN.

3.2 CONTEXT LENGTH AND MASKING RATIO

The Delphyne architecture requires careful tuning of key training parameters, like the masking ratio during pre-training. While vision transformers use around 60% (He et al., 2022), language models use 15%, and prior pre-trained time-series models range from 30% to 50% (Goswami et al., 2024; Woo et al., 2024). This ratio is crucial as it affects input context length, impacting generalization and fine-tuning. We perform ablation studies to explore the impact of masking ratios and context lengths on training efficiency.

Ablation 1. The first experiment explores how varying pre-training context lengths affects both pre-training and fine-tuning performance. We train small- and medium-size autoregressive transformer decoders on synthetic Wavelet data with context lengths of $\{16, 32, 64, 128\}$ (details in Appendix I.1). After convergence, we assess zero-shot NLL forecast with a fixed context length of 32. Fine-

tuning is performed with varying amounts of data, consistently using a context length of 32. Table 3 reports the NLL for zero-shot and fine-tuning. While pre-training with a context length of 32 yields the best zero-shot performance, a longer context length of 64, 128 improves fine-tuning, especially with fewer fine-tuning (10-100) samples. This suggests that for effective fine-tuning, pre-trained time-series models benefit from longer context lengths during pre-training.

Table 3: NLL(\downarrow) for zero-shot and fine-tuning with varying sample sizes. Pretraining on a context length of 32 yields the best zero-shot performance, while pretraining on a longer context length of 128 improves fine-tuning, especially with 10-100 samples.

Model	Zero-Shot	1 Sample	10 Samples	100 Samples	1000 Samples
Small-16	-0.0449	-0.1189	-0.1523	-0.1824	-0.1870
Small-32	-0.0978	-0.0842	-0.1681	-0.1873	-0.1898
Small-64	-0.0808	-0.1418	-0.1684	-0.1861	-0.1853
Small-128	-0.0842	-0.1287	-0.1825	-0.1907	-0.1918
Medium-16	-0.0483	-0.0893	-0.1542	-0.1767	-0.1897
Medium-32	-0.1330	-0.1486	-0.1673	-0.1792	-0.1847
Medium-64	-0.0793	-0.1146	-0.1612	-0.1873	-0.1875
Medium-128	-0.1020	-0.1113	-0.1711	-0.1843	-0.1899

Ablation 2. We vary the maximum masking ratio in $\{0.25, 0.5, 0.99\}$ and observe the effects of the resulting model. We use a transformer encoder and vary on Wavelet data (Appendix I.2). We evaluate the model’s fine-tuning performance by NLL of various forecast length, see Table 4. When masking less aggressively, the model consistently performs well across various forecast lengths. This aligns with our earlier findings, as less aggressive masking implicitly exposes the model to longer context lengths during pre-training, leading to improved fine-tuning performance.

During model pre-training, we apply a masking ratio to each variate, sampled from a beta-binomial distribution with $\alpha = 5$ and $\beta = 10$, the average masking ratio is around 30%. Each variate is masked independently, enabling our model to better adapt to nowcasting scenarios where variates and covariates may have different lookback window lengths.

3.3 TRAINING ON MULTIVARIATE DATA

Multivariate time-series modeling poses unique challenges, particularly in capturing correlations between variates. Nie et al. (2023) analyze channel-mixing versus channel-independence approaches, finding that the latter improves adaptability and generalization. Many pre-trained models for multivariate time series adopt channel-independence (Goswami et al., 2024; Ekambaram et al., 2024), while others focus solely on univariate time series (Ansari et al., 2024; Das et al., 2024; Rasul et al., 2023). Recently, Woo et al. (2024) introduce any-variate attention (Appendix A), which flattens multivariates into univariates and captures inter-variate correlations via a specialized bias term. We conduct experiments on synthetic Wavelet data to compare these design choices.

Ablation 3. We model two scenarios: one where the Wavelet data across rows are correlated, and another where they are uncorrelated. In the correlated scenario, the time-series data are generated using the same Wavelet function, differing only by additive Gaussian noise. In the uncorrelated scenario, the data are generated using different Wavelet functions, see Appendix I.3 for details.

Table 5 shows the results. Multivariate models significantly outperform univariate approaches for correlated rows of Wavelet data, underscoring the importance of capturing inter-variable dependencies. Channel-mixing shows superior performance in zero-shot settings and with smaller training samples, but only when training and forecasting with correlated Wavelet data. However, when data rows are uncorrelated, channel-mixing performs worse than other two models. Given

Table 4: NLL(\downarrow) for varying pre-training masking ratios.

	Sample Size	Masking Ratio		
		0.25	0.5	0.99
Pred. Len. 32	1	-0.441	-0.187	0.416
	10	-0.394	-0.071	0.496
	100	-0.580	-0.391	0.321
	1000	-0.666	-0.662	-0.676
Pred. Len. 64	1	-0.263	-0.077	0.122
	10	-0.236	-0.077	0.144
	100	-0.296	-0.158	0.088
	1000	-0.318	-0.314	-0.318
Pred. Len. 96	1	0.015	0.081	0.132
	10	-0.022	0.072	0.144
	100	-0.006	0.044	0.128
	1000	-0.020	-0.023	-0.023

Table 5: NLL(\downarrow) for zero-shot and fine-tuning with varying sample sizes, for different modeling multivariate methods.

Model	Zero-Shot	1 Sample	10 Samples	100 Samples	1000 Samples
Cor.	Univariate	-0.0978	-0.0842	-0.1681	-0.1873
	Channel Mixing	-0.1531	-0.1650	-0.1797	-0.1913
	Any-variate Attention	-0.1513	-0.1507	-0.1794	-0.1892
Uncorr.	Univariate	-0.0978	-0.0842	-0.1681	-0.1873
	Channel Mixing	-0.0928	-0.1323	-0.1722	-0.1892
	Any-variate Attention	-0.0922	-0.1386	-0.1879	-0.1879

that Delphyne is trained on both strongly and weakly correlated financial data such as the returns of stocks across various sectors, it employs an any-variate attention mechanism. This mechanism enables the integration of cross-channel information without forcibly mixing variate data. Unlike Woo et al. (2024), we do not intentionally create multivariate data rows across different datasets.

3.4 OUTPUT DISTRIBUTION

For probability forecasting, previous studies usually assume a fixed output distribution (Salinas et al., 2020a). However, when the data presents varying distributions and supports, relying on a single distribution may be insufficient. Woo et al. (2024) propose a mixture of a Student’s T-distribution, Log-normal, Gaussian, and Negative Binomial, which introduces asymmetry into the forecasted distribution and demonstrates improved results. We conduct an additional experiment studying the effect of various distributions.

Ablation 4. With a fixed training regime and transformer backbone, we measure a stock return’s NLL (Sec. 5.1) across three output distributions: a single distribution, a Student’s T mixture, and a mixture of different distributions as in Woo et al. (2024), which we call MOIRAI’s Mixture (see details in Appendix I.4). Fig. 4 shows that the Student’s T mixture performs similarly to MOIRAI’s Mixture on measuring stock returns. On the other hand, a single distribution underperforms both. For simplicity (Occam’s Razor), we choose the Student’s T mixture as the output distribution, with further discussion in the probability quantification experiment (Sec. 5.4).

4 TRAINING DETAILS

4.1 TRAINING DATA

We include both publicly available data and financial data in Delphyne’s training, allowing Delphyne to generalize well to daily time-series forecast tasks as well as financial time-series tasks. We give a brief overview of our two sources of training data.

LOTSA Data (Woo et al., 2024) is the largest publicly available dataset for pre-training large time-series models, containing 231 billion observations across domains like energy, transport, climate, CloudOps, web, sales, nature, economics, finance, and healthcare. It aggregates most open source time-series datasets. An overview is provided in Appendix B.1.

Financial Data Our financial dataset contains data for companies, stocks, ETFs, currencies (exchange rates), and commodities. Further, to handle multiple frequencies, we create daily datasets and monthly datasets. To ensure that there is no lookahead bias in our downstream tasks, we pre-train with data only until the end of 2019. We provide a detailed breakdown of the dataset in Appendix B.2.

Sampling The LOTSA dataset is significantly imbalanced, necessitating subsampling to ensure more balanced representation during training. We carefully identify the few datasets that dominate in size and reduce their likelihood of being sampled to avoid overrepresentation. For any dataset, we first compute the total number of observations (across samples, variates, and timesteps) within the dataset, $|\mathcal{D}_k| = \sum_{i=1}^M \sum_{j=1}^{l+k} T_{i,j}$. Then, we normalize the scores to sum to one. We cap the weighting to be at least 0.001 which we normalize again to obtain the final probability of sampling a dataset. Overall, our training data consists of 85% from LOTSA and 15% from financial data (Table 6). We sample the number of variates (≤ 128) using a beta-binomial distribution ($\alpha = 2$ and $\beta = 5$).

Table 6: Sampling dataset probability (%) across LOTSA domains and finance data.

LOTSA	Energy 17.8	Transport 25.5	CloudOps 8.6	Climate 11.9	Econ/fin 5.7	Web 6.1	Sales 5.4	Nature 3.9	Healthcare 0.2	Total 85
Finance Data	ETFs 2.8	Tickers 2.8	Commodities 0.3	Currency 0.9	Stock 2.8	Company 1.8	Intraday Bars 2.8			Total 15

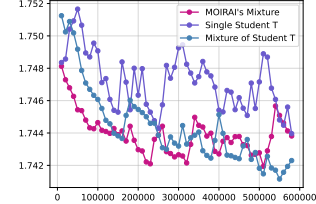


Figure 4: Stock NLL performance on three different output distributions.

Unlike other models (Woo et al., 2024; Goswami et al., 2024) that involve complex preprocessing like packing, concatenation, or augmentation, our approach is streamlined. We only apply subsampling and truncate time to 512×32 timesteps. For the ease of normalization, we exclude entries with fewer than five observations or uniform values after forecast and missing masking. This keeps the training data robust and optimizes model performance without excessive preprocessing.

4.2 MODEL PARAMETERS

We train Delphyne with 12 layers and 768-dimensional attention shared across 12 heads, with a maximum width of 3072. Dropout is set to 0.2, and the model is trained on negative log-likelihood (NLL) loss. We pretrained for 1 million gradient updates with a fixed patch size of 32 and a sequence length of 512×32 steps. Using a batch size of 256, we optimize with AdamW (learning rate = $1e-4$, weight decay = 0.1, $\beta_1 = 0.9$, $\beta_2 = 0.98$) and apply a learning rate scheduler with 10,000 steps of linear warmup and cosine annealing to $1e-5$. Training was conducted on 8 H100 GPUs over 4 days with mixed-precision (bf16) (Kalamkar et al., 2019) for speed.

5 EXPERIMENTS

We train three models for downstream evaluations. Delphyne trained on the LOTSA dataset (Woo et al., 2024), Delphyne trained on finance data only, and Delphyne trained with all finance and LOTSA dataset, which we define as Delphyne-L, Delphyne-F, and Delphyne-A, respectively. We compare the zero-shot (ZS) forecasts and fine-tuning (FT) performances on standard short-term and long-term time-series forecasting tasks, probabilistic quantification, anomaly detection tasks, as well as the finance forecast tasks for stock risk analysis, stock volatility modeling, intraday traded volume modeling, and company revenue nowcasting.

5.1 FINANCIAL TASKS

Stocks. While a commonly evaluated task for finance is forecasting the returns, modeling the distribution of stock returns is equally important where it can be used for stress-testing scenarios, and conducting risk analysis (Tepelyan & Gopal, 2023). To test the performance of different methods on this task, we use the daily stock returns of 14 major stocks from SPX Index from 2021-01-04 to 2023-12-29. For fine-tuning, we use data from 1996-07-01 to 2019-12-31 for training, 2020-01-02 to 2020-12-31 for validation with a context length of 252.

Since most methods, except MOIRAI (Woo et al., 2024), forecast point estimates, we conduct two experiments: forecasting next-day stock returns' variance (volatility) to compare MSE, and evaluating NLL (Negative Log Likelihood) for the forecasted returns distribution. We also benchmark against GARCH with Student's T, a standard financial baseline (Tepelyan & Gopal, 2023). For PatchTST (Nie et al., 2023), we adapt the output to a mixture of four Student's T distributions.

Table 7 and 8 show the overall results. The NLL metrics indicate that while utilizing only financial data in pre-training brings best zero-shot performance (Delphyne-F), Delphyne-A achieves the best results after fine-tuning. The MSE for variance forecasts shows that Delphyne models outperform others and perform better in zero-shot than after fine-tuning. We hypothesize that the dataset's high noise leads to overfitting during fine-tuning. Additional evaluation of coverage statistics (a measure of the model's calibration performance) confirms that Delphyne models achieve the best performance (Appendix D.1).

Table 7: Likelihood results for next-day stock returns risk analysis.

Model	NLL ZS	NLL FT
Delphyne-A	1.762	1.741
Delphyne-F	1.750	1.746
Delphyne-L	1.775	1.757
MOIRAI	1.776	1.788
GARCH	-	1.752
PatchTST	-	1.751

Table 8: MSE for next-day stock squared returns (variance).

Model	MSE ZS	MSE FT
Delphyne-A	37.792	37.810
Delphyne-F	37.653	38.616
Delphyne-L	37.591	38.246
MOIRAI	41.428	40.502
MOMENT	46.006	37.785
TTM	44.918	44.360
PatchTST	-	51.705
GARCH	-	41.517

Table 9: MSE for bars log-volume data. (78 timestep predictions of 5-minute intervals)

Model	MSE ZS	MSE FT
Delphyne-A	0.728	0.551
Delphyne-F	0.965	0.530
Delphyne-L	0.930	0.557
MOIRAI	0.767	0.620
MOMENT	0.775	0.838
TTM	0.714	0.601
PatchTST	-	0.534
Avg past values	0.602	-

Table 10: Nowcasting results for zero-shot vs. fine-tuning for company sales growth

Model	MAE ZS	MAE FT
Delphyne-A	0.099	0.071
Delphyne-F	0.128	0.079
Delphyne-L	0.101	0.073
MOIRAI	0.091	0.093
Baseline	0.100	-

Bars. We use the intraday bars data, which contains the log of volume traded (log-volume) in five-minute intervals to test the different methods’ performance in long-sequence modeling. For 4 different ETFs, we use the past 15 days data (context length 15×78) to forecast the log-volume in the next day’s trading hours (e.g., forecast length of 78) and compare their mean-squared errors.

Table 9 shows the results for 2021-01-04 to 2021-01-11. For fine-tuning, data from 2008-01-24 to 2019-12-30 is used for training, and 2019-12-31 to 2020-12-31 for validation. All Delphyne models significantly improve metrics after fine-tuning, effectively capturing the seasonal component in bar log-volume data. Delphyne-A-ZS outperforms Delphyne-F-ZS and Delphyne-L-ZS due to the data’s seasonal nature, similar to electricity and weather datasets. However, with fine-tuning, Delphyne-F achieves the best performance across all methods.

Nowcasting Company Revenue. We use consumer transaction data to test nowcasting performance (e.g., when we have contemporaneous data), forecasting year-over-year (YoY) sales growth for 211 U.S. companies based on 1) previous quarter’s YoY sales growth, 2) previous YoY growth in transactions, and 3) current quarter’s YoY growth in transactions. Due to the quarterly nature, the context length is short (4-8). We make rolling forecasts for Q3 2022 to Q1 2023. For fine-tuning, data from 2018 Q1 to 2021 Q1 is used for training, and 2021 Q2 to 2022 Q2 for validation. We compare against a statistical baseline built by the providers of the consumer transaction data and MOIRAI (Woo et al., 2024). Table 10 shows MSE results: Delphyne-A with fine-tuning outperforms all methods, and Delphyne-L ranks second despite not seeing the data during pre-training. We attribute this to Delphyne-L’s independent masking of variates during pre-training, which enhances handling of contemporaneous data for nowcasting.

5.2 SHORT-TERM FORECASTING ON MONASH DATASET

We conduct an evaluation using the Monash dataset (Godahewa et al., 2021), which spans multiple domains like demand forecasting, traffic, and weather, with various data granularities. We follow the train-test split outlined in Woo et al. (2024), evaluating performance only on the hold-out test set to ensure a fair in-distribution comparison for Delphyne-L and Delphyne-A, whose pre-training datasets contain training sets of Monash data. We partition out the same forecast length as the test set, used as validation data for finetuning the model. We report both zero-shot and finetuning results. For zero-shot, we fix context length equals 500 and report the test performance. For fine-tuning, we search context length in $\{100, 300, 500, 1000, 2000\}$ and the learning rate in $\{5e-5, 1e-5\}$.

We compare Delphyne with statistical baselines, supervised ML baselines, foundation models, and LLM-based models. Full MAE result for comparison is in Table 16 and comparison across versions of Delphyne is in Table 17. Fig. 5 and Fig. 6 provide the aggregate results of normalized MAE (the geometric mean of the MAE of each dataset divided by the MAE of the Naive approach).

In zero-shot performance, Delphyne-F, trained solely on finance data, slightly outperforms the Naive model and the other three benchmarks. Since Monash is out-of-distribution for Delphyne-F, a decline in performance is expected. In contrast, Delphyne-L achieves a lower MAE than Delphyne-A, likely because that Delphyne-A’s training data contains finance data and may introduce negative transfer effects. After fine-tuning, both Delphyne-A and Delphyne-L show similar performance, rivaling the best model, MOIRAI (Woo et al., 2024).

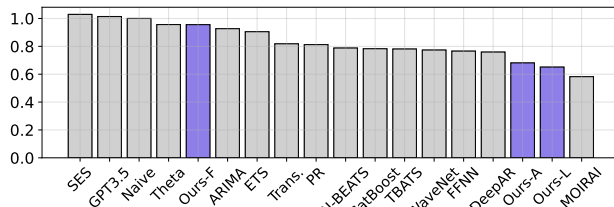


Figure 5: Aggregated geometric mean of normalized MAEs on the Monash Time-Series Forecasting Benchmark. On average, Delphyne zero-shot models perform better than existing models, falling into second place behind MOIRAI.

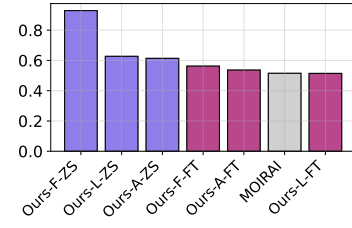


Figure 6: Aggregated geometric mean of normalized MAEs for Delphyne zero-shot (ZS) and fine-tuned(FT) models.

5.3 OUT-OF-DISTRIBUTION LONG-TERM FORECASTING

For long-term forecasting, we evaluate Delphyne and benchmarks on popular datasets with forecast lengths of 96, 192, 336, and 720. We use the standard ETT datasets, weather (Zhou et al., 2021) and electricity(ECL) dataset (Trindade, 2015) . See Appendix E for experiment details.

We report the average performance across various forecast lengths for zero-shot, linear probing, fine-tuning, and full-shot methods in Table 11, with the full results provided in Table 24. Admittedly, Delphyne-A underperforms compared to TTM, MOIRAI, and other foundation models in zero-shot settings. This may be attributed to its use of fixed patch sizes rather than dynamic adaptation and Delphyne’s training on the negative log-likelihood of a Student’s-T mixture distribution, which is optimized for financial tasks. However, Delphyne-A demonstrates strong performance after fine-tuning, a crucial step for improving out-of-distribution forecasting. Its architectural design and training paradigm make it particularly adaptable.

We provide a comparison of Delphyne models in Table 25 . Delphyne-A significantly outperforms Delphyne-L on ETTm1 and ETTh1 with a 720-forecast length, with no observed negative transfer. This may be due to the shared seasonality trends between ETT and financial (bars) data. However, both models achieve similar performance after fine-tuning.

Table 11: Average MAE and MSE across prediction lengths $\{96, 192, 336, 720\}$ for Delphyne and other baseline methods. The best are highlighted in **bold** and the runner-up is underlined.

	Zero-shot				Linear-Probing			Fine-tuned			Full-Shot			
	TTM	MOIRAI	TimesFM	Delphyne-A-ZS	MOMENT	GPT4TS	Delphyne-A-FT	PatchTST	Dlinear	TimesNet	FEDFormer	Stationary		
ETTh1														
MSE	0.402	0.434	0.476	0.449	0.418	0.428	0.440	<u>0.413</u>	0.423	0.457	0.440	0.460	0.570	
MAE	-	0.439	0.451	0.450	0.436	0.426	0.441	<u>0.431</u>	0.437	0.449	0.460	0.537		
ETTh2														
MSE	0.327	<u>0.346</u>	0.404	0.375	0.352	0.355	0.352	0.330	0.431	0.414	0.437	0.526		
MAE	-	0.382	0.406	0.404	0.395	0.395	0.356	<u>0.379</u>	0.447	0.427	0.449	0.516		
ETTm1														
MSE	0.338	0.382	0.420	0.501	0.354	0.352	0.364	<u>0.351</u>	0.357	0.400	0.448	0.481		
MAE	-	0.388	0.408	0.429	0.391	0.383	0.365	0.381	<u>0.379</u>	0.406	0.452	0.456		
ETTm2														
MSE	0.264	0.272	0.350	0.323	0.256	0.266	0.250	<u>0.255</u>	0.267	0.291	0.305	0.306		
MAE	-	0.321	0.353	0.363	<u>0.270</u>	0.326	0.257	0.315	0.334	0.333	0.350	0.347		
ECL														
MSE	<u>0.160</u>	0.188	0.156	0.202	0.165	0.167	0.170	0.162	0.166	0.193	0.214	0.193		
MAE	-	0.274	<u>0.246</u>	0.293	0.260	0.263	0.203	0.253	0.264	0.295	0.327	0.296		
Weather														
MSE	0.233	0.235	0.232	0.369	0.230	0.237	0.221	<u>0.226</u>	0.249	0.259	0.309	0.288		
MAE	-	0.263	<u>0.257</u>	0.348	0.261	0.271	0.235	0.264	0.300	0.286	0.360	0.314		

5.4 PROBABILITY QUANTIFICATION

We assess probability forecasting on six datasets spanning the energy, transport, climate, and sales domains, using a rolling evaluation setup where the stride matches the forecast length. Additional experiment setups, comparison methods, and full results are shown in Appendix F.

We report the Continuous Ranked Probability Score (CRPS) and Mean Scaled Interval Score (MSIS) metrics (definitions in Appendix F) in Table 12, and additional deterministic metrics are shown in Table 27. Delphyne-A’s zero-shot performance is slightly below that of MOIRAI (Woo et al., 2024), particularly in terms of CRPS metrics. However, after fine-tuning, Delphyne-A shows significant improvement, achieving the best results across various datasets. We suspect that we outperform in MSIS likely due to Delphyne-A modeling having a heavier-tailed distribution using a mixture of Student’s T distributions, but there is still room in selecting a more expressive distribution to improve CRPS, as distributions can be specific to each dataset.

5.5 ANOMALY DETECTION

We measure adjusted F1 score for the anomaly detection task, on 44 time-series datasets for the UCR anomaly detection archive, in comparison to popular full-shot models and foundation model MOMENT with anomaly detection head (Goswami et al., 2024). Experiment setups and full results are in Appendix G.

The aggregated F1 score is provided in Fig. 7. Delphyne-A’s versatility allows it to adapt well to anomaly detection tasks after fine-tuning, achieving second place overall in anomaly detection tasks.

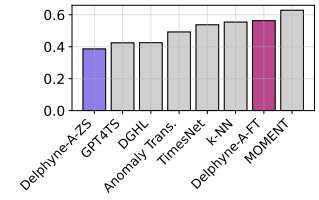


Figure 7: Aggregated Adjusted F1 Score for Delphyne-A vs. comparison baselines.

Table 12: Full results for probabilistic forecasting experiments. The best results are highlighted in **bold**, and the second best results are underlined. (The baseline results are taken from Woo et al. (2024).)

	Zero-shot		Finetuned		Full-shot			Baseline	
	Delphyne-A-ZS	MOIRAI	Delphyne-A-FT	PatchTST	TIDE	TFT	DeepAR	AutoARIMA	Seasonal Naive
Electricity	CRPS	0.159	0.055	0.140 \pm 0.005	0.052 \pm 0.00	0.048\pm0.00	0.050 \pm 0.00	0.065 \pm 0.01	0.327
	MSIS	29.293	6.172	21.820 \pm 1.383	<u>5.744\pm0.12</u>	5.672\pm0.08	6.278 \pm 0.24	6.893 \pm 0.82	29.412
Solar	CRPS	0.905	0.419	1.306 \pm 0.103	0.518 \pm 0.09	0.420\pm0.00	0.446 \pm 0.03	0.431 \pm 0.01	1.055
	MSIS	2.733	7.011	2.029\pm0.520	8.447 \pm 1.59	13.754 \pm 0.32	8.057 \pm 3.51	11.181 \pm 0.67	25.849
Walmart	CRPS	0.093	0.093	0.083 \pm 0.001	0.082 \pm 0.01	0.077\pm0.00	0.087 \pm 0.00	0.121 \pm 0.00	0.124
	MSIS	4.741	8.421	4.559\pm0.289	6.005 \pm 0.21	6.258 \pm 0.12	8.718 \pm 0.10	12.502 \pm 0.03	9.888
Weather	CRPS	0.064	0.041	0.042 \pm 0.005	0.059 \pm 0.01	0.054 \pm 0.00	0.043 \pm 0.00	0.132 \pm 0.01	0.252
	MSIS	6.080	<u>5.136</u>	4.467\pm0.053	7.759 \pm 0.49	8.095 \pm 1.74	7.791 \pm 0.44	21.651 \pm 17.34	19.805
Istanbul Traffic	CRPS	0.149	0.116	0.212 \pm 0.015	0.112 \pm 0.00	0.110 \pm 0.01	0.110\pm0.01	0.108\pm0.00	0.589
	MSIS	9.989	4.461	4.328 \pm 0.536	3.813\pm0.09	4.752 \pm 0.17	<u>4.057\pm0.44</u>	4.094 \pm 0.31	16.317
Turkey Power	CRPS	0.046	<u>0.040</u>	0.035\pm0.001	0.054 \pm 0.01	0.046 \pm 0.01	0.039 \pm 0.00	0.066 \pm 0.02	0.116
	MSIS	<u>6.269</u>	6.766	5.384\pm0.346	8.978 \pm 0.51	8.579 \pm 0.52	7.943 \pm 0.31	13.520 \pm 1.17	14.863

6 RELATED WORK

Transformer-based Time-series Modeling. Transformers have become a powerful backbone for time-series analysis (Wen et al., 2023). Many studies enhance attention mechanisms to handle longer context lengths in time-series data (Zhou et al., 2021; 2022). Nie et al. (2023) show that segmenting time-series data into patches as tokens improves performance and captures representations effectively for forecasting. Similarly, Liu et al. (2024d) treat independent time series as tokens to capture inter-correlations, enhancing multivariate forecasting.

Time-series Foundation Models. Building on the rise of LLMs, recent research has explored the potential of large deep learning models for time-series analysis. One approach adapts existing pre-trained language models for time-series tasks through prompting (Zhou et al., 2023; Jin et al., 2024; Chang et al., 2023; Gruver et al., 2023; Liu et al., 2024c), while another focuses on training foundation models specifically on time-series data (Woo et al., 2024; Das et al., 2024; Goswami et al., 2024; Ekambaram et al., 2024). Both strategies seek to develop a single model trained on large-scale, cross-domain data, capable of addressing multiple forecasting tasks, in contrast to full-shot methods that require training a separate model for each dataset. Our work is closely related to foundation models (See Appendix J), with several architectural modifications for financial domains.

Transfer Learning and Distribution Shift in Time-series domains. The negative transfer effect is widely studied in the transfer learning literature, but remains less explored in the context of pre-training models for time-series modeling. This effect can be viewed through the lens of distribution shifts within training and testing time-series datasets. Several studies have proposed methods to address distribution shifts in time-series tasks (Fan et al., 2023; Kim et al., 2022; Liu et al., 2024a;b). Our work differs from the distribution shift literature; we aim to develop a pre-trained time-series model capable of rapidly adapting to downstream tasks through few-shot fine-tuning.

7 CONCLUSIONS

We illustrate the presence of negative transfer effect in pre-trained time-series models especially when pre-trained with time-series data from various domains, contrasting them with LLMs for language tasks. Our experiments emphasize the role of fine-tuning to counter this effect which helps pre-trained time-series models to adapt to diverse downstream tasks with few training samples and minimal iterations. We introduce various architectural modifications, supported by ablation studies, to handle continuous, noisy, multivariate and multifrequency nature of time-series data. Delphyne is the first pre-trained model excelling in both general time-series and diverse financial and economic tasks such as nowcasting.

REFERENCES

Alexander Alexandrov, Konstantinos Benidis, Michael Bohlke-Schneider, Valentin Flunkert, Jan Gasthaus, Tim Januschowski, Danielle C. Maddix, Syama Rangapuram, David Salinas, Jasper Schulz, Lorenzo Stella, Ali Caner Türkmen, and Yuyang Wang. GluonTS: Probabilistic and

Neural Time Series Modeling in Python. *Journal of Machine Learning Research*, 21(116):1–6, 2020. URL <http://jmlr.org/papers/v21/19-820.html>.

Abdul Fatir Ansari, Lorenzo Stella, Caner Turkmen, Xiyuan Zhang, Pedro Mercado, Huibin Shen, Oleksandr Shchur, Syama Syndar Rangapuram, Sebastian Pineda Arango, Shubham Kapoor, Jasper Zschiegner, Danielle C. Maddix, Hao Wang, Michael W. Mahoney, Kari Torkkola, Andrew Gordon Wilson, Michael Bohlke-Schneider, and Yuyang Wang. Chronos: Learning the Language of Time Series. *arXiv preprint arXiv:2403.07815*, 2024.

Gustavo Silva Araujo and Wagner Piazza Gaglianone. Machine Learning Methods for Inflation Forecasting in Brazil: New Contenders versus Classical Models. *Latin American Journal of Central Banking*, 4(2):100087, 2023. doi: 10.1016/j.latcb.2023.100087.

V. Assimakopoulos and K. Nikolopoulos. The Theta Model: A Decomposition Approach to Forecasting. *International Journal of Forecasting*, 16(4):521–530, 2000. doi: 10.1016/S0169-2070(00)00066-2.

Tim Bollerslev. Generalized Autoregressive Conditional Heteroskedasticity, journal = Journal of Econometrics. 31(3):307–327, 1986. doi: 10.1016/0304-4076(86)90063-1.

David Campos, Miao Zhang, Bin Yang, Tung Kieu, Chenjuan Guo, and Christian S. Jensen. LightTS: Lightweight Time Series Classification with Adaptive Ensemble Distillation. *Proc. ACM Manag. Data*, 1(2):171:1–171:27, 2023. doi: 10.1145/3589316.

Ching Chang, Wen-Chih Peng, and Tien-Fu Chen. Llm4ts: Two-stage fine-tuning for time-series forecasting with pre-trained llms. *arXiv preprint arXiv:2308.08469*, 2023.

Zihan Chen, Lei Zheng, Cheng Lu, Jialu Yuan, and Di Zhu. ChatGPT Informed Graph Neural Network for Stock Movement Prediction. *SSRN Electronic Journal*, 2023. doi: 10.2139/ssrn.4464002.

Abhimanyu Das, Weihao Kong, Rajat Sen, and Yichen Zhou. A decoder-only foundation model for time-series forecasting. In Ruslan Salakhutdinov, Zico Kolter, Katherine Heller, Adrian Weller, Nuria Oliver, Jonathan Scarlett, and Felix Berkenkamp (eds.), *Proceedings of the 41st International Conference on Machine Learning*, volume 235 of *Proceedings of Machine Learning Research*, pp. 10148–10167. PMLR, 21–27 Jul 2024. URL <https://proceedings.mlr.press/v235/das24c.html>.

Anna Veronika Dorogush, Vasily Ershov, and Andrey Gulin. CatBoost: Gradient Boosting with Categorical Features Support. *CoRR*, abs/1810.11363, 2018. URL <http://arxiv.org/abs/1810.11363>.

Vijay Ekambaram, Arindam Jati, Pankaj Dayama, Sumanta Mukherjee, Nam H. Nguyen, Wesley M. Gifford, Chandra Reddy, and Jayant Kalagnanam. Tiny Time Mixers (TTMs): Fast Pre-trained Models for Enhanced Zero/Few-Shot Forecasting of Multivariate Time Series, 2024. URL <https://arxiv.org/abs/2401.03955>.

Stefan Elfwing, Eiji Uchibe, and Kenji Doya. Sigmoid-Weighted Linear Units for Neural Network Function Approximation in Reinforcement Learning. *Neural Networks (Special issue on reinforcement learning)*, 107:3–11, 2018. doi: 10.1016/j.neunet.2017.12.012.

Patrick Emami, Abhijeet Sahu, and Peter Graf. BuildingsBench: A Large-Scale Dataset of 900K Buildings and Benchmark for Short-Term Load Forecasting. In *Thirty-seventh Conference on Neural Information Processing Systems Datasets and Benchmarks Track*, 2023. URL <https://openreview.net/forum?id=c5rqd6PZn6>.

Wei Fan, Pengyang Wang, Dongkun Wang, Dongjie Wang, Yuanchun Zhou, and Yanjie Fu. Dish-TS: A General Paradigm for Alleviating Distribution Shift in Time Series Forecasting. In *Proceedings of the Thirty-Seventh AAAI Conference on Artificial Intelligence and Thirty-Fifth Conference on Innovative Applications of Artificial Intelligence and Thirteenth Symposium on Educational Advances in Artificial Intelligence, AAAI’23/IAAI’23/EAAI’23*. AAAI Press, 2023. doi: 10.1609/aaai.v37i6.25914.

Azul Garza and Max Mergenthaler-Canseco. Timegpt-1. *arXiv preprint arXiv:2310.03589*, 2023.

Tilmann Gneiting and Adrian E Raftery. Strictly Proper Scoring Rules, Prediction, and Estimation. *Journal of the American Statistical Association*, 102(477):359–378, 2007.

R. W. Godahewa, C. Bergmeir, G. I. Webb, R. Hyndman, and P. Montero-Manso. Monash Time Series Forecasting Archive. In *Thirty-fifth Conference on Neural Information Processing Systems Datasets and Benchmarks Track (Round 2)*, 2021. URL <https://openreview.net/forum?id=wEc1mgAju->.

Achintya Gopal. Neuralfactors: A novel factor learning approach to generative modeling of equities. In *Proceedings of the 5th ACM International Conference on AI in Finance*, pp. 99–107, 2024.

Mononito Goswami, Cristian Ignacio Challu, Laurent Callot, Lenon Minorics, and Andrey Kan. Unsupervised Model Selection for Time Series Anomaly Detection. In *The Eleventh International Conference on Learning Representations*, 2023. URL https://openreview.net/forum?id=gOZ_pKANaPW.

Mononito Goswami, Konrad Szafer, Arjun Choudhry, Yifu Cai, Shuo Li, and Artur Dubrawski. MOMENT: A Family of Open Time-series Foundation Models, 2024. URL <https://arxiv.org/abs/2402.03885>.

Nate Gruver, Marc Finzi, Shikai Qiu, and Andrew G Wilson. Large Language Models Are Zero-Shot Time Series Forecasters. In A. Oh, T. Naumann, A. Globerson, K. Saenko, M. Hardt, and S. Levine (eds.), *Advances in Neural Information Processing Systems*, volume 36, pp. 19622–19635. Curran Associates, Inc., 2023. URL https://proceedings.neurips.cc/paper_files/paper/2023/file/3eb7ca52e8207697361b2c0fb3926511-Paper-Conference.pdf.

Kaiming He, Xinlei Chen, Saining Xie, Yanghao Li, Piotr Dollár, and Ross Girshick. Masked Autoencoders Are Scalable Vision Learners. In *2022 IEEE/CVF Conference on Computer Vision and Pattern Recognition (CVPR)*, pp. 15979–15988, 2022. doi: 10.1109/CVPR52688.2022.01553.

Matthew D. Hoffman and Andrew Gelman. The No-U-Turn Sampler: Adaptively Setting Path Lengths in Hamiltonian Monte Carlo. *Journal of Machine Learning Research*, 15(47):1593–1623, 2014. URL <http://jmlr.org/papers/v15/hoffman14a.html>.

Noah Hollmann, Samuel Müller, Katharina Eggensperger, and Frank Hutter. TabPFN: A Transformer That Solves Small Tabular Classification Problems in a Second. In *The Eleventh International Conference on Learning Representations*, 2023. URL https://openreview.net/forum?id=cp5PvcI6w8_.

Blanka Horvath, Aitor Muguruza, and Mehdi Tomas. Deep learning volatility. *arXiv preprint arXiv:1901.09647*, 2019.

Rob J Hyndman. Errors on Percentage Errors, 4 2014. URL <https://robjhyndman.com/hyndtsight/smape/>.

Rob J Hyndman and Anne B Koehler. Another Look at Measures of Forecast Accuracy. *International Journal of Forecasting*, 22(4):679–688, 2006.

Ming Jin, Shiyu Wang, Lintao Ma, Zhixuan Chu, James Y. Zhang, Xiaoming Shi, Pin-Yu Chen, Yuxuan Liang, Yuan-Fang Li, Shirui Pan, and Qingsong Wen. Time-LLM: Time Series Forecasting by Reprogramming Large Language Models. In *The Twelfth International Conference on Learning Representations*, 2024. URL <https://openreview.net/forum?id=Unb5CVpta>.

Dhiraj Kalamkar, Dheevatsa Mudigere, Naveen Mellemudi, Dipankar Das, Kunal Banerjee, Sasikanth Avancha, Dharm Teja Vooturi, Nataraj Jammalamadaka, Jianyu Huang, Hector Yuen, et al. A study of bfloat16 for deep learning training. *arXiv preprint arXiv:1905.12322*, 2019.

Taesung Kim, Jinhee Kim, Yunwon Tae, Cheonbok Park, Jang-Ho Choi, and Jaegul Choo. Reversible Instance Normalization for Accurate Time-Series Forecasting against Distribution Shift. In *International Conference on Learning Representations*, 2022. URL <https://openreview.net/forum?id=cGDAkQo1C0p>.

Haoxin Liu, Harshavardhan Kamarthi, Lingkai Kong, Zhiyuan Zhao, Chao Zhang, and B. Aditya Prakash. Time-series forecasting for out-of-distribution generalization using invariant learning. In *Forty-first International Conference on Machine Learning*, 2024a. URL <https://openreview.net/forum?id=SMUXPVKUBg>.

Haoxin Liu, Shangqing Xu, Zhiyuan Zhao, Lingkai Kong, Harshavardhan Kamarthi, Aditya B. Sasanur, Megha Sharma, Jiaming Cui, Qingsong Wen, Chao Zhang, and B. Aditya Prakash. Time-MMD: Multi-domain multimodal dataset for time series analysis. In *The Thirty-eight Conference on Neural Information Processing Systems Datasets and Benchmarks Track*, 2024b. URL <https://openreview.net/forum?id=fuD0h4R1IL>.

Haoxin Liu, Zhiyuan Zhao, Jindong Wang, Harshavardhan Kamarthi, and B Aditya Prakash. Lst-prompt: Large language models as zero-shot time series forecasters by long-short-term prompting. *arXiv preprint arXiv:2402.16132*, 2024c.

Xu Liu, Yutong Xia, Yuxuan Liang, Junfeng Hu, Yiwei Wang, LEI BAI, Chao Huang, Zhenguang Liu, Bryan Hooi, and Roger Zimmermann. LargeST: A Benchmark Dataset for Large-Scale Traffic Forecasting. In *Thirty-seventh Conference on Neural Information Processing Systems Datasets and Benchmarks Track*, 2023. URL <https://openreview.net/forum?id=1o0w3oyhFW>.

Yong Liu, Tengge Hu, Haoran Zhang, Haixu Wu, Shiyu Wang, Lintao Ma, and Mingsheng Long. iTransformer: Inverted Transformers Are Effective for Time Series Forecasting. In *The Twelfth International Conference on Learning Representations*, 2024d. URL <https://openreview.net/forum?id=JePfAI8fah>.

Yuxin Liu, Jimin Lin, and Achintya Gopal. Neuralbeta: Estimating beta using deep learning. *arXiv preprint arXiv:2408.01387*, 2024e.

Alejandro Lopez-Lira and Yuehua Tang. Can chatgpt forecast stock price movements? return predictability and large language models. *arXiv preprint arXiv:2304.07619*, 2023.

Spyros Makridakis, Evangelos Spiliotis, and Vassilios Assimakopoulos. The M4 Competition: 100,000 time series and 61 forecasting methods. *International Journal of Forecasting*, 36(1): 54–74, 2020.

Haitao Mao, Zhikai Chen, Wenzhuo Tang, Jianan Zhao, Yao Ma, Tong Zhao, Neil Shah, Mikhail Galkin, and Jiliang Tang. Position: Graph Foundation Models Are Already Here. In Ruslan Salakhutdinov, Zico Kolter, Katherine Heller, Adrian Weller, Nuria Oliver, Jonathan Scarlett, and Felix Berkenkamp (eds.), *Proceedings of the 41st International Conference on Machine Learning*, volume 235 of *Proceedings of Machine Learning Research*, pp. 34670–34692. PMLR, 21–27 Jul 2024. URL <https://proceedings.mlr.press/v235/mao24a.html>.

S. Mouatadid, P. Orenstein, G. E. Flaspoehler, M. Oprescu, J. Cohen, F. Wang, S. E. Knight, M. Geogdzayeva, S. J. Levang, E. Fraenkel, and L. Mackey. SubseasonalclimateUSA: A Dataset for Subseasonal Forecasting and Benchmarking. In *Thirty-seventh Conference on Neural Information Processing Systems Datasets and Benchmarks Track*, 2023. URL <https://openreview.net/forum?id=pWkrU6raMt>.

Samuel Müller, Noah Hollmann, Sebastian Pineda Arango, Josif Grabocka, and Frank Hutter. Transformers Can Do Bayesian Inference. In *International Conference on Learning Representations*, 2022. URL <https://openreview.net/forum?id=KSugKcbNf9>.

Yuqi Nie, Nam H Nguyen, Phanwadee Sinthong, and Jayant Kalagnanam. A Time Series is Worth 64 Words: Long-term Forecasting with Transformers. In *The Eleventh International Conference on Learning Representations*, 2023. URL <https://openreview.net/forum?id=Jbdc0vTOcol>.

Boris N. Oreshkin, Dmitri Carpow, Nicolas Chapados, and Yoshua Bengio. N-BEATS: Neural Basis Expansion Analysis for Interpretable Time Series Forecasting. In *International Conference on Learning Representations*, 2020. URL <https://openreview.net/forum?id=r1ecqn4YwB>.

Youngsuk Park, Danielle Maddix, François-Xavier Aubet, Kelvin Kan, Jan Gasthaus, and Yuyang Wang. Learning Quantile Functions without Quantile Crossing for Distribution-Free Time Series Forecasting. In *International Conference on Artificial Intelligence and Statistics*, pp. 8127–8150. PMLR, 2022.

Alessio Petrozziello, Luigi Troiano, Angela Serra, Ivan Jordanov, Giuseppe Storti, Roberto Tagliafiri, and Michele La Rocca. Deep Learning for Volatility Forecasting in Asset Management. *Soft Computing*, 26(17):8553–8574, 2022. doi: 10.1007/s00500-022-07161-1.

Kashif Rasul, Arjun Ashok, Andrew Robert Williams, Arian Khorasani, George Adamopoulos, Rishika Bhagwatkar, Marin Biloš, Hena Ghonia, Nadhir Hassen, Anderson Schneider, Sahil Garg, Alexandre Drouin, Nicolas Chapados, Yuriy Nevmyvaka, and Irina Rish. Lag-Llama: Towards Foundation Models for Time Series Forecasting. In *R0-FoMo: Robustness of Few-shot and Zero-shot Learning in Large Foundation Models*, 2023. URL <https://openreview.net/forum?id=jYluzCLFDM>.

David Salinas, Valentin Flunkert, Jan Gasthaus, and Tim Januschowski. DeepAR: Probabilistic Forecasting with Autoregressive Recurrent Networks. *International Journal of Forecasting*, 36(3):1181–1191, 2020a. doi: 10.1016/j.ijforecast.2019.07.001.

David Salinas, Valentin Flunkert, Jan Gasthaus, and Tim Januschowski. DeepAR: Probabilistic Forecasting with Autoregressive Recurrent Networks. *International Journal of Forecasting*, 36(3):1181–1191, 2020b. doi: 10.1016/j.ijforecast.2019.07.001.

Noam Shazeer. Glu variants improve transformer. *arXiv preprint arXiv:2002.05202*, 2020.

Jianlin Su, Murtadha Ahmed, Yu Lu, Shengfeng Pan, Wen Bo, and Yunfeng Liu. RoFormer: Enhanced transformer with Rotary Position Embedding. *Neurocomput.*, 568(C), March 2024. doi: 10.1016/j.neucom.2023.127063.

Ruslan Tepelyan and Achintya Gopal. Generative Machine Learning for Multivariate Equity Returns. In *Proceedings of the Fourth ACM International Conference on AI in Finance*, ICAIF '23, pp. 159–166, New York, NY, USA, 2023. Association for Computing Machinery. doi: 10.1145/3604237.3626884.

Artur Trindade. ElectricityLoadDiagrams20112014. UCI Machine Learning Repository, 2015.

Aäron van den Oord, Sander Dieleman, Heiga Zen, Karen Simonyan, Oriol Vinyals, Alex Graves, Nal Kalchbrenner, Andrew W. Senior, and Koray Kavukcuoglu. WaveNet: A Generative Model for Raw Audio. *CoRR*, abs/1609.03499, 2016. URL <http://arxiv.org/abs/1609.03499>.

Mike Van Ness, Huibin Shen, Hao Wang, Xiaoyong Jin, Danielle C Maddix, and Karthick Gopal-swamy. Cross-frequency time series meta-forecasting. *arXiv preprint arXiv:2302.02077*, 2023.

J. Wang, J. Jiang, W. Jiang, C. Han, and W. X. Zhao. Towards Efficient and Comprehensive Urban Spatial-Temporal Prediction: A Unified Library and Performance Benchmark. *arXiv preprint arXiv:2304.14343*, 2023.

Zehong Wang, Zheyuan Zhang, Chuxu Zhang, and Yanfang Ye. Subgraph Pooling: Tackling Negative Transfer on Graphs. In Kate Larson (ed.), *Proceedings of the Thirty-Third International Joint Conference on Artificial Intelligence*, IJCAI-24, pp. 5153–5161. International Joint Conferences on Artificial Intelligence Organization, 8 2024a. doi: 10.24963/ijcai.2024/570. Main Track.

Zhixian Wang, Qingsong Wen, Chaoli Zhang, Liang Sun, Leandro Von Krannichfeldt, Shirui Pan, and Yi Wang. Benchmarks and Custom Package for Electrical Load Forecasting, 2024b. URL <https://openreview.net/forum?id=gjB7qqPJbv>.

Zirui Wang, Zihang Dai, Barnabás Póczos, and Jaime Carbonell. Characterizing and Avoiding Negative Transfer. In *2019 IEEE/CVF Conference on Computer Vision and Pattern Recognition (CVPR)*, pp. 11285–11294, 2019. doi: 10.1109/CVPR.2019.01155.

Qingsong Wen, Tian Zhou, Chaoli Zhang, Weiqi Chen, Ziqing Ma, Junchi Yan, and Liang Sun. Transformers in Time Series: A Survey. In Edith Elkind (ed.), *Proceedings of the Thirty-Second International Joint Conference on Artificial Intelligence, IJCAI-23*, pp. 6778–6786. International Joint Conferences on Artificial Intelligence Organization, 8 2023. doi: 10.24963/ijcai.2023/759.

Gerald Woo, Chenghao Liu, Akshat Kumar, and Doyen Sahoo. Pushing the limits of pre-training for time series forecasting in the cloudops domain. *arXiv preprint arXiv:2310.05063*, 2023.

Gerald Woo, Chenghao Liu, Akshat Kumar, Caiming Xiong, Silvio Savarese, and Doyen Sahoo. Unified Training of Universal Time Series Forecasting Transformers. In Ruslan Salakhutdinov, Zico Kolter, Katherine Heller, Adrian Weller, Nuria Oliver, Jonathan Scarlett, and Felix Berkenkamp (eds.), *Proceedings of the 41st International Conference on Machine Learning*, volume 235 of *Proceedings of Machine Learning Research*, pp. 53140–53164. PMLR, 21–27 Jul 2024. URL <https://proceedings.mlr.press/v235/woo24a.html>.

Haixu Wu, Tengge Hu, Yong Liu, Hang Zhou, Jianmin Wang, and Mingsheng Long. Timesnet: Temporal 2d-variation modeling for general time series analysis. In *The Eleventh International Conference on Learning Representations*, 2023. URL https://openreview.net/forum?id=ju_Uqw3840q.

Ruimin Xiong, Yunchang Yang, Di He, Kai Zheng, Shuxin Zheng, Chen Xing, Huishuai Zhang, Yanyan Lan, Liwei Wang, and Tieyan Liu. On Layer Normalization in the Transformer Architecture. In Hal Daumé III and Aarti Singh (eds.), *Proceedings of the 37th International Conference on Machine Learning*, volume 119 of *Proceedings of Machine Learning Research*, pp. 10524–10533. PMLR, 13–18 Jul 2020. URL <https://proceedings.mlr.press/v119/xiong20b.html>.

Hsiang-Fu Yu, Nikhil Rao, and Inderjit S Dhillon. Temporal regularized matrix factorization for high-dimensional time series prediction. In D. Lee, M. Sugiyama, U. Luxburg, I. Guyon, and R. Garnett (eds.), *Advances in Neural Information Processing Systems*, volume 29. Curran Associates, Inc., 2016. URL https://proceedings.neurips.cc/paper_files/paper/2016/file/85422afb467e9456013a2a51d4dff702-Paper.pdf.

Xinli Yu, Zheng Chen, Yuan Ling, Shujing Dong, Zongyi Liu, and Yanbin Lu. Temporal data meets llm-explainable financial time series forecasting. *arXiv preprint arXiv:2306.11025*, 2023.

Haoyi Zhou, Shanghang Zhang, Jieqi Peng, Shuai Zhang, Jianxin Li, Hui Xiong, and Wancai Zhang. Informer: Beyond Efficient Transformer for Long Sequence Time-Series Forecasting. *Proceedings of the AAAI Conference on Artificial Intelligence*, 35(12):11106–11115, May 2021. doi: 10.1609/aaai.v35i12.17325.

Tian Zhou, Ziqing Ma, Qingsong Wen, Xue Wang, Liang Sun, and Rong Jin. FEDformer: Frequency Enhanced Decomposed Transformer for Long-term Series Forecasting. In Kamalika Chaudhuri, Stefanie Jegelka, Le Song, Csaba Szepesvari, Gang Niu, and Sivan Sabato (eds.), *Proceedings of the 39th International Conference on Machine Learning*, volume 162 of *Proceedings of Machine Learning Research*, pp. 27268–27286. PMLR, 17–23 Jul 2022. URL <https://proceedings.mlr.press/v162/zhou22g.html>.

Tian Zhou, Peisong Niu, Xue Wang, Liang Sun, and Rong Jin. One Fits All: Power General Time Series Analysis by Pretrained LM. In *Thirty-seventh Conference on Neural Information Processing Systems*, 2023. URL <https://openreview.net/forum?id=gMS6FVZvmF>.

A ANY-VARIATE ATTENTION

Any-variate attention is first proposed by Woo et al. (2024) to allow binary attention biases to encode variate indices for a flattened multi-variate time series. The attention score between the (i, m) -th query and (j, n) -th query (j and i represent the time-steps, and n and m encode the variate index) is calculated as the following:

$$E_{ij,mn} = (\mathbf{W}^Q \mathbf{x}_{i,m})^T \mathbf{R}_{i-j} (\mathbf{W}^K \mathbf{x}_{j,n}) + u^{(1)} * \mathbb{1}_{\{m=n\}} + u^{(2)} * \mathbb{1}_{\{m \neq n\}}, \quad (3)$$

$$A_{ij,mn} = \frac{\exp(E_{ij,mn})}{\sum_{k,o} \exp(E_{ik,mo})}, \quad (4)$$

where $\mathbf{W}^Q \mathbf{x}_{i,m}, \mathbf{W}^K \mathbf{x}_{j,n} \in \mathbb{R}^{d_h}$ are the query and key vectors. $u^{(1)}$ and $u^{(2)}$ are learnable scalars as the attention biases. These binary attention biases component enables differentiation between variates, satisfies permutation equivariance and invariance with respect to variate ordering, and is scalable to any number of variates.

B PRE-TRAINING DATA

B.1 LOTSA

1. **BuildingsBench** BuildingsBench (Emami et al., 2023) comprises of datasets detailing energy consumption in residential and commercial buildings. These include the real-world BDG-2 datasets, Low Carbon London, SMART, IDEAL, Sceaux, and Borealis, which capture energy usage from diverse sources. BuildingsBench introduces the Buildings-900K dataset, a large-scale simulation of 900K buildings, while both the training and testing splits are included in LOTSA. Electricity is omitted in LOTSA and used for out-of-distribution evaluation.
2. **ClimateLearn** This dataset includes both ERA5 and CMIP6 (Nie et al., 2023), which contain various climate-related variables like temperature and humidity across different pressure levels. In LOTSA, we observe that ERA5 and CMIP6 are divided into several data folders across different years. To address this, we reduce the probability of their appearance by treating all directories spanning multiple years as single datasets.
3. **CloudOps** CloudOps-TSF, introduced by Woo et al. (2023), provides three large-scale time series datasets that capture variables like CPU and memory utilization. Only training dataset is included in LOTSA.
4. **GluonTS (Alexandrov et al., 2020)** For this dataset, only Taxi, Uber TLC Daily, Uber TLC Hourly, Wiki-Rolling, and M5 are included. The rest of the datasets are already included in the Monash dataset.
5. **LargeST (Liu et al., 2023)** This dataset contains traffic datasets from California Department of Transportation Performance Measurement System (PeMS). PeMS includes PEMS03, PEMS04, PEMS07, PEMS08, PEMS Bay, and the well-known Traffic dataset.
6. **LibCity (Wang et al., 2023)** This is a collection of urban spatio-temporal datasets, while the spatial aspect is dropped.
7. **Monash** The Monash Time Series Forecasting Repository (Godahewa et al., 2021) is a comprehensive collection of diverse time series datasets. The test data for each dataset is the final horizon as the test set, while the forecast horizon is defined for each individual dataset. LOTSA includes the training data of Monash dataset, holding out the testing for in-distribution evaluation. Several datasets are included entirely in LOTSA: London Smart Meters, Wind Farms, Wind Power, Solar Power, Oikolab Weather, Covid Mobility, Extended Web Traffic, Kaggle Web Traffic Weekly, M1 Yearly, M1 Quarterly, M3 Yearly, M3 Quarterly, M4 Yearly, M4 Quarterly, Tourism Yearly. In our experiment evaluation, we do not fine-tune Delphyne on several datasets in Monash, due to that their training data is very short (< 20 time steps) after splitting the data into test data and validation data.

BO1	HO1	QS1
CC1	JO1	SB1
CL1	KC1	SI1
CO1	KO1	S
CT1	LA1	TZT1
CU1	LB1	UXA1
C	LP1	W
FN1	MO1	XB1
GC1	NG1	XW1
HG1	PL1	

Table 13: List of commodities tickers

8. **ProEnFo** ProEnFo (Wang et al., 2024b) is a dataset for load forecasting. Its data contains various covariates such as temperature, humidity, and wind speed.
9. **SubseasonalClimateUSA (Mouatadid et al., 2023)** This dataset offers climate time series data for subseasonal forecasting. LOTSA contains Subseasonal Precipitation, containing precipitation data from 1948 to 1978, and Subseasonal, which includes both precipitation and temperature data from 1979 to 2023.
10. **Other** LOTSA also contains datasets from miscellaneous sources, spanning from energy, econ/finance, sales and healthcare. Refer to Table 17 in Woo et al. (2024) for details.

B.2 FINANCIAL DATA

By design, our data sampling samples time-series from the same dataset with the same sample ID; because of this, some of our datasets have the same time-series but are used in different contexts (sampled with different time series).

1. **Single Currency Daily** This dataset includes 12 exchange rates, and each exchange rate is treated as a separate sample. For each exchange rate, we include the time series of the exchange rate and its returns, forward rates, and implied volatilities. We use 1W, 1M, 3M, 6M, 9M, 1Y, 18M, and 2Y for the tenors, and 0.1, 0.15, 0.25, 0.35, 0.5, 0.65, 0.75, 0.85, and 0.9 for the deltas. This dataset trains the model to properties across the spot, forward, and volatility surface.
2. **Joint Currencies Daily** This data includes 68 currency pairs, the exchange rate and returns are the time series. This dataset is to allow our model to learn correlations across currencies; to this end, there is only one sample.
3. **Currencies Monthly** This dataset includes 43 exchange rates, and each exchange rate is treated as a separate sample. We use the same columns as in Single Currency Daily except the returns are monthly returns.
4. **Commodities Daily** This dataset includes 29 commodities, and each commodity is treated as a separate sample. Similar to exchange rates, we include the price and returns of the commodity, and the implied volatilities for 1M, 2M, 3M, 6M, 1Y, 18M, and 2Y for the tenors, and 90%, 95.0%, 97.5%, 100.0%, 102.5%, 105.0%, and 110.0% for the moneyness.
5. **Commodities Monthly** This dataset is identical to ‘Commodities Daily’ except that the data is resampled to monthly level where we take monthly returns and the last value per month for the rest of the columns.
6. **Joint Stock Returns** Similar to ‘Joint Currencies Daily’, this dataset is to allow our model to learn correlations across stocks. This data includes the returns of 10,511 stocks. To ensure the correlations learned are more meaningful, we partitioned the stocks into 53 exchanges.
7. **Daily ETFs Returns** Similar to ‘Joint Stock Returns’, this dataset is to allow our model to learn correlations across ETFs. This data includes the returns of 28,837 ETFs. To ensure the correlations learned are more meaningful, we partitioned the stocks into 76 exchanges.

is_sg&a_expense	net_income	is_cogs_to_fe_and_pp_and_g
is_sales_and_services_revenues	is_other_operating_expenses	is_cog_and_services_sold
is_operating_expn	ebit	sales_rev_turn
ebitda	short_and_long_term_debt	bs_tot_asset
bs_cur_liab	bs_cur_asset_report	bs_gross_fix_asset
total_equity	bs_pfd_eqty_&_hybrid_cptl	bs_inventories
bs_cash_near_cash_item	bs_lt_invest	bs_net_fix_asset
bs_acct_note_rcv	cash_and_marketable_securities	enterprise_value
net_debt	sales_to_net_fix_asset	gross_profit
num_of_employees	gross_margin	historical_market_cap
avg_age_of_assets_in_years	cf_cap_expend_prpty_add	cf_cash_from_inv_act

Table 14: List of company financials fields

observed_sales	observed_transactions	observed_unique_customers
average_transaction_value	transactions_per_customer	sales_per_customer

Table 15: List of consumer transactions fields

8. **Company Data** Similar to ‘Single Currency Daily’, this dataset is to allow our model to learn correlation across stock features. This data includes 10,511 stocks. For variates, we include stock returns, volume traded, quarterly company financials, consumer transaction data, forward rates for the same tenors as ‘Single Currency Daily’, and implied volatilities for the same moneynesses as ‘Commodities Daily’ as well as 80% and 120% moneyness.
9. **Intraday Bars** We include 15,817 global securities and for each five-minute interval (bar), we include the open, high, low, and closing price, the volume traded, and the number of trades. Since the securities have different open and close hours, to normalize the data, we drop specific five-minute intervals (a specify day of the week and time) for which the ticker has had zero trades through its life.

C MONASH TIME SERIES FORECAST

C.1 COMPARISON METHODS

Pre-trained Models. For pre-trained models we report the zero-shot performance of MOIRAI (Woo et al., 2024). MOIRAI is a unified pre-trained foundation model for time-series analysis. Across the three versions of MOIRAI, we report its performance across MOIRAI_{Base}, which is roughly the same amount of parameters as our Delphyne models.

Baselines. Several traditional and statistical methods serve as the reported baseline for Monash, using the last observed value for the forecast. SES (Single Exponential Smoothing) applies a weighted average to past observations, with exponentially decreasing weights for older data points. Theta (Assimakopoulos & Nikolopoulos, 2000) fits θ -lines with exponential smoothing. Exponential Smoothing (ETS) is also a traditional statistical method.

Non-deep Methods. The non-deep learning methods include CatBoost (gradient boosting on decision trees) (Dorogush et al., 2018), (DHR)-ARIMA (dynamic harmonic regression), PR.

Deep Methods. Methods that include training neural networks include N-BEATS (Oreshkin et al., 2020), feed-forward neural network (FFMM), DeepAR (Salinas et al., 2020b), N-BEATS (Oreshkin et al., 2020), WaveNet (van den Oord et al., 2016) and Transformer (Trans).

GPT3.5 & Llama2. GPT3.5 and Llama2 are two versions of LLMTTime. For GPT-3.5, we report the reproduced results by Woo et al. (2024), as well as the original results by Gruver et al. (2023) run on Llama2.

C.2 FULL COMPARISON RESULTS

See Table 16 for a comparison across baselines and Table 17 for comparison across different versions of Delphyne.

Table 16: Full results of Monash Time Series Forecasting Benchmark. MAE is reported. The best result is in **bold**. **”Aggregated”** means that we take the geometric mean of the MAE of each dataset divided by the MAE of the Naive approach (for zero-shot models only, fine-tuned performances are reported in Table 17).

Dataset	Delphyne-A-ZS	Delphyne-A-FT	MOIRAI	Naive	SES	Theta	TBATS	ETS	(DHR-)ARIMA	PR	CatBoost	FFNN	DeepAR	N-BEATS	WaveNet	Trans.	GPT3.5	LLaMA2
M1 Monthly	2153.37	-	2068.63	2707.75	2259.04	2166.18	2237.50	1905.28	2080.13	2088.25	2052.32	2162.58	1860.81	1820.37	2184.42	2723.88	2562.84	-
M3 Monthly	649.77	-	658.17	837.14	743.41	623.71	630.59	626.46	654.8	692.97	732	692.48	728.81	648.6	699.3	798.38	877.97	-
M3 Other	202.44	-	198.62	278.43	277.83	215.35	189.42	194.98	193.02	234.43	318.13	240.17	247.56	221.85	245.29	239.24	300.30	-
M4 Monthly	507.43	560.47	594.23	671.42	661.60	580.42	654.49	651.36	675.26	614.29	614.29	579.48	655.42	700.44	655.27	700.27	655.27	-
M4 Weekly	378.36	306.06	328.08	347.09	336.82	333.32	296.15	335.66	321.61	293.21	364.65	338.37	351.78	277.73	359.46	378.89	518.44	-
M4 Daily	223.54	181.89	192.66	180.83	178.27	178.6	193.26	179.67	181.93	231.36	177.91	299.79	190.44	189.47	201.08	266.52	-	-
M4 Hourly	948.85	211.93	209.87	1218.06	1218.06	1220.97	386.27	3358.10	1310.85	257.39	285.35	385.49	886.37	425.75	393.63	320.54	576.06	-
Tourism Quarterly	9489.13	-	17190.86	15840.10	15014.19	7656.49	3972.42	3999.52	1047.47	1047.47	1047.47	8860.97	9518.37	9644.69	9171.12	9521.67	16978.86	9311.98
Tourism Monthly	2615.26	-	2888.41	2802.06	558.83	558.10	469.09	508.08	5804.51	6022.21	5530.71	6071.62	5135.74	5714.69	6903.02	5950.22	5608.86	3145.48
CIF 2016 (E+5)	4.67	-	5.39	5.78	5.81	7.15	8.56	6.42	4.69	5.63	6.08	14.96	32.00	6.79	59.98	40.58	5.99	6.84
Aus. Elec.	235.49	248.62	201.39	659.6	659.6	655.14	370.74	1282.99	1045.92	247.18	241.77	258.76	302.41	213.83	227.75	231.45	760.81	560.48
Bitcoin(E+8)	2.15	1.44	1.87	0.78	5.53	5.53	0.82	1.10	3.62	0.66	1.93	258.95	1.06	2.46	2.61	1.74	8.57	-
Pedestrian Counts	32.69	44.50	22.17	170.88	139.87	170.96	222.38	154.55	635.16	34.84	46.41	47.8	66.04	46.46	47.8	57.77	65.92	-
Vehicle Trips	17.68	21.85	31.42	24.98	30.76	21.21	30.95	30.97	27.24	22.61	22.92	23	28.16	24.15	28.01	31.48	-	-
KDD cup	30.87	29.96	39.09	42.13	42.04	42.06	39.2	44.88	52.2	36.85	34.82	37.16	48.99	49.1	37.08	44.46	42.72	-
Weather	2.05	1.79	1.8	2.36	2.24	2.51	2.3	2.35	2.45	8.17	2.51	2.09	2.02	2.34	2.29	2.17	2.09	-
NN5 Daily	3.57	3.65	4.26	8.26	6.63	3.8	3.7	3.72	4.41	5.47	4.22	4.06	4.77	3.97	4.17	7.10	6.67	-
NN5 Weekly	15.60	14.28	16.12	16.71	15.66	15.17	14.98	15.38	14.98	15.94	15.03	14.69	14.19	19.34	20.34	15.76	15.60	-
Carparts	0.65	0.47	0.65	0.55	0.53	0.58	0.56	0.56	0.41	0.53	0.39	0.39	0.98	0.4	0.39	0.44	-	-
FRED-MD	3806.16	2907.86	2679.29	2825.67	2798.22	3492.84	1989.97	2041.92	2957.11	8921.99	2475.68	2339.57	4624.36	2557.8	2508.4	4666.04	2804.64	1781.41
Traffic Hourly	0.02	0.02	0.03	0.03	0.04	0.04	0.03	0.05	0.02	0.02	0.01	0.01	0.02	0.02	0.02	0.01	0.02	0.02
Traffic Weekly	1.13	1.13	1.14	1.19	1.12	1.13	1.17	1.14	1.22	1.13	1.17	1.15	1.18	1.11	1.2	1.42	1.15	1.15
Rideshare	1.12	1.19	1.29	1.29	1.29	1.29	1.29	1.29	1.29	1.23	1.22	1.22	1.22	1.23	1.25	1.28	1.28	-
Hospital	19.08	-	19.4	24.07	21.76	18.54	17.43	17.97	19.6	19.24	19.17	22.86	18.25	19.35	36.19	25.68	22.75	-
COVID Deaths	174.35	137.76	113.31	353.71	353.71	321.32	96.29	85.59	87.77	347.98	475.15	144.14	201.98	158.81	1049.48	408.66	653.31	66.14
Temperature Rain	6.27	5.14	5.08	9.39	8.18	8.22	7.14	8.21	7.19	6.13	6.76	5.56	5.37	7.28	5.81	5.24	6.37	-
Sunspot	3.51	0.41	0.41	3.93	4.93	4.93	2.97	3.95	2.97	3.85	2.77	7.07	0.77	14.47	0.17	0.13	5.07	0.28
Sageen	24.41	21.55	24.4	21.5	21.5	21.49	22.46	20.69	20.69	22.48	25.24	22.98	20.21	27.27	22.17	20.95	34.84	23.01
US Births	462.16	442.71	614.3	1152.67	1192.20	586.93	399	417.93	526.33	574.92	441.7	557.87	422	504.4	452.87	1374.99	638.82	-
Aggregated	0.68	-	0.58	1.0	1.03	0.96	0.78	0.91	0.93	0.81	0.78	0.77	0.76	0.79	0.77	0.82	1.01	-

Table 17: Delphyne model results of Monash Time Series Forecasting Benchmark. MAE is reported; for fine-tuning, the MAE is taken over 3 experimental runs and we report the mean \pm std. The best result is in **bold**. **”Aggregated (Fine-tune)”** means that we take the geometric mean of the MAE of each fine-tuned dataset divided by the MAE of the Naive approach.

Dataset	Delphyne-L-ZS	Delphyne-F-ZS	Delphyne-A-ZS	Delphyne-L-FT	Delphyne-F-FT	Delphyne-A-FT
M1 Monthly	2252.507	2298.433	2153.370	-	-	-
M3 Monthly	643.874	817.461	649.765	-	-	-
M3 Other	209.257	493.340	202.444	-	-	-
M4 Monthly	620.923	697.144	597.434	569.709 \pm 7.662	563.145 \pm 9.496	560.472\pm2.022
M4 Weekly	340.878	379.246	378.363	296.282\pm4.909	319.959 \pm 38.095	306.055 \pm 5.195
M4 Daily	210.110	201.094	223.536	174.349\pm0.727	182.327 \pm 3.155	181.884 \pm 5.742
M4 Hourly	234.718	1369.664	218.845	263.368 \pm 16.039	331.591 \pm 29.941	211.930\pm0.657
Tourism Quarterly	9268.650	17143.935	9487.128	-	-	-
Tourism Monthly	2458.334	6074.311	2615.256	2360.693\pm123.850	2460.906 \pm 277.598	2488.407 \pm 205.380
CIF 2016 (E+6)	5.408	2.826	4.670	-	-	-
Aus. Elec.	203.034	1795.900	235.490	199.854\pm0.200	235.263 \pm 5.601	248.615 \pm 0.959
Bitcoin (E+8)	1.928	1.871	2.152	1.255 \pm 0.174	1.185\pm0.861	1.437 \pm 0.332
Pedestrian Counts	44.367	170.285	52.987	41.917\pm0.532	58.494 \pm 5.365	44.505 \pm 1.217
Vehicle Trips	18.327	20.227	17.682	-	-	-
KDD cup	30.045	35.768	30.868	30.029 \pm 0.019	28.822\pm0.110	29.964 \pm 0.039
Weather	2.053	2.495	2.052	1.776\pm0.014	1.807 \pm 0.036	1.792 \pm 0.010
NN5 Daily	3.596	3.622	3.574	3.566 \pm 0.044	3.474\pm0.017	3.648 \pm 0.063
NN5 Weekly	14.899	15.945	14.999	14.109\pm0.045	14.189 \pm 0.047	14.280 \pm 0.087
Carparts	0.656	0.662	0.652	-	-	-
FRED-MD	2868.493	3510.298	3806.159	2720.094\pm101.289	4008.423 \pm 198.970	2907.856 \pm 200.807
Traffic Hourly	0.018	0.038	0.018	0.015\pm0.000	0.016 \pm 0.000	0.017 \pm 0.001
Traffic Weekly	1.121	1.163	1.125	1.108\pm0.007	1.123 \pm 0.005	1.131 \pm 0.010
Rideshare	1.256	1.676	1.123	1.221 \pm 0.010	1.110\pm0.001	1.111 \pm 0.001
Hospital	19.029	22.427	19.081	-	-	-
COVID Deaths	154.175	385.451	174.354	135.791\pm21.305	180.857 \pm 23.128	137.716 \pm 4.510
Temperature Rain	6.794	7.515	6.267	5.341 \pm 0.160	5.482 \pm 0.112	5.142\pm0.006
Sunspot	3.163	9.458	3.507	0.328 \pm 0.035	0.455 \pm 0.072	0.410 \pm 0.015
Sageen	24.281	23.757	25.410	24.780 \pm 0.088	23.258 \pm 0.209	21.552\pm0.169
US Births	443.349	462.390	463.157	365.175\pm42.777	425.495 \pm 9.022	442.705 \pm 0.801
Aggregated	0.623	0.929	0.626	0.514	0.562	0.536
Fine-tune	-	-	-	-	-	-

D FINANCIAL TASKS

The hyperparameters we tuned are in Table 18. Note, for MOMENT (Goswami et al., 2024), we use patch length of 8 and the context length to 512 since these are fixed by the model. Similarly, for TTM (Ekambaran et al., 2024), we used a context length of 512 since this is fixed by the model; we also used a head dropout of 0.7 (as suggested in the paper).

Table 18: Hyperparameter search values for financial tasks.

Hyperparameter		Values
Delphyne	learning rate dropout	$\{1e-5, 5e-4, 1e-4\}$ $\{0.1, 0.2, 0.3\}$
MOIRAI	learning rate patch size	$\{1e-5, 5e-4, 1e-4\}$ $\{16, 32\}$
TTM	learning rate	$\{1e-5, 5e-4, 1e-4, 1e-3\}$
PatchTST	patch size hidden size dropout	$\{1, 4, 16, 32\}$ $\{64, 128, 256\}$ $\{0.0, 0.1, 0.2\}$

D.1 CALIBRATION ANALYSIS FOR STOCKS TASK

In addition to evaluating the models with NLL, we can also evaluate the coverage statistics: **given a forecasted quantile q , what percentage of the observations are less than that value?** In Table 19, we present the results. We see that Delphyne-A-FT performs the best or second-best in nearly all of the quantiles.

Table 19: Results of stock risk analysis for zero-shot versus fine-tuning with stocks coverage statistic. We **bold** the results that are closest in absolute error to the optimal coverage.

Model	Q10	Q25	Q50	Q75	Q90
Optimal	0.100	0.250	0.500	0.750	0.900
Delphyne-A-ZS	0.109	0.239	<u>0.502</u>	<u>0.749</u>	0.892
Delphyne-F-ZS	<u>0.104</u>	0.252	0.515	0.777	0.907
Delphyne-L-ZS	0.097	0.238	0.525	0.790	0.906
Delphyne-A-FT	0.106	<u>0.246</u>	0.501	0.750	0.900
Delphyne-F-FT	0.086	0.216	0.487	0.768	<u>0.903</u>
Delphyne-L-FT	0.089	0.216	0.510	0.794	0.916
MOIRAI-ZS	0.108	0.215	0.445	0.732	0.877
MOIRAI-FT	0.083	0.205	0.493	0.794	0.917
GARCH	0.111	0.269	0.561	0.790	0.913
PatchTST	0.114	0.264	0.509	0.748	0.896

Table 20: Full results for zero-shot versus fine-tuning for predicting next-day stock squared-returns (variance) data. MSE is reported; for fine-tuning, the MSE is taken over 3 experimental runs and we report the mean \pm std.

Model	MSE ZS	MSE FT
Delphyne-A	37.792	37.810 ± 0.105
Delphyne-F	<u>37.653</u>	38.616 ± 1.566
Delphyne-L	37.591	38.246 ± 0.598
MOIRAI	41.428	40.502 ± 0.046
MOMENT	46.006	37.935 ± 0.179
TTM	44.918	44.360 ± 0.004
PatchTST	-	51.705 ± 11.467
GARCH	41.517	-

Table 21: Full results for zero-shot versus fine-tuning for next-day stock-returns risk analysis. NLL is reported; for fine-tuning, the NLL is taken over 3 experimental runs and we report the mean \pm std.

Model	NLL ZS	NLL FT
Delphyne-A	1.762	1.741\pm0.002
Delphyne-F	1.750	1.746 \pm 0.001
Delphyne-L	1.775	1.757 \pm 0.005
MOIRAI	1.776	1.788 \pm 0.001
GARCH	1.752	-
PatchTST	-	1.751 \pm 0.005

Table 22: Full results for zero-shot versus fine-tuning for predicting bars log-volume data (longer horizon, 78 timesteps prediction for 5-minute intervals). MSE is reported; for fine-tuning, the MSE is taken over 3 experimental runs and we report the mean \pm std.

Model	MSE ZS	MSE FT
Delphyne-A	0.728	0.551 \pm 0.017
Delphyne-F	0.965	0.530\pm0.01
Delphyne-L	0.930	0.557 \pm 0.002
MOIRAI	0.765	0.621 \pm 0.003
MOMENT	0.775	0.838 \pm 0.028
TTM	0.714	0.600 \pm 0.001
PatchTST	-	<u>0.534</u>
Last Value	0.602	-

Table 23: Nowcasting results for zero-shot vs. fine-tuning for company sales growth data. MAE is reported; for fine-tuning, the MAE is taken over 3 experimental runs and we report the mean \pm std.

Model	MAE ZS	MAE FT
Delphyne-A	0.099	0.071\pm0.002
Delphyne-F	0.128	0.079 \pm 0.003
Delphyne-L	0.101	0.073 \pm 0.001
MOIRAI	0.091	0.093 \pm 0.001
Baseline	0.100	-

E LONG-TERM FORECASTING EXPERIMENT

For fine-tuning Delphyne, we use a learning rate of 5e-5, dropout of 0.2, batch size of 64, and a linear warmup for the learning rate of 50 steps. For all datasets, we use a context length of 1000. We use early-stopping based on the validation loss. Due to Electricity and Weather being large datasets, we randomly sample 32×500 rows from the validation set for early-stopping. For long-term forecasting experiment, we do not conduct any additional hyperparameter searching, although that could lead to improved performances.

E.1 COMPARISON METHODS

Zero-Shot Methods. For zero-shot methods, we report TTM_A , the best and largest model presented in Ekambaram et al. (2024). Since the authors have only published models with a forecast length of 96, we are limited to reporting the MSE based on their reported results. For MOIRAI (Woo et al., 2024), we again report the performance of $\text{MOIRAI}_{\text{Base}}$, which has similar number of parameters as our model. For TimesFM (Das et al., 2024), we follow their demonstration¹ and report the MSE and MAE results for their checkpoint "google/timesfm-1.0-200m" in Huggingface.

Linear-Probing. We directly report the linear probing results from MOMENT's experiments (Goswami et al., 2024), which include baseline results for both Time-LLM (Jin et al., 2024) and GPT4TS (Zhou et al., 2023).

Full-Shot. The full-shot results are obtained from Goswami et al. (2024). Within the full-shot results, PatchTST (Nie et al., 2023), DLinear (Elfwing et al., 2018), TimesNet (Wu et al., 2023), FEDFormer (Zhou et al., 2022), Stationary (Zhou et al., 2023), LightTS (Campos et al., 2023) and N-BEATS (Oreshkin et al., 2020) are reported.

E.2 FULL COMPARISON RESULTS

Table 24 shows an comparison across different models and Table 25 shows the comparison across different versions of Delphyne.

Table 24: Zero-shot and Full-shot Results for Delphyne and Other Models

Dataset	Horizon	Zero-shot						Linear-Probing						Fine-tuned						Full-shot													
		TTM		MOIRAI		TimesFM		Delphyne-A-ZS		MOMENT		Time-LLM		GPT4TS		Delphyne-A-FT		PatchTST		DLinear		TimesNet		FEDFormer		Stationary		LightTS		N-BEATS			
		MSE	MAE	MSE	MAE	MSE	MAE	MSE	MAE	MSE	MAE	MSE	MAE	MSE	MAE	MSE	MAE	MSE	MAE	MSE	MAE	MSE	MAE	MSE	MAE	MSE	MAE	MSE	MAE				
ETTh1	96	0.359	-	0.384	0.402	0.405	0.432	0.398	0.417	0.387	0.410	0.408	0.429	0.376	0.397	0.376	0.390	0.375	0.399	0.375	0.399	0.375	0.398	0.402	0.379	0.419	0.513	0.491	0.424	0.432	0.399	0.428	
	192	0.389	-	0.425	0.429	0.459	0.432	0.440	0.444	0.410	0.426	-	-	0.416	0.418	0.432	0.440	0.413	0.421	0.429	0.416	0.436	0.429	0.428	0.448	0.521	0.492	0.475	0.462	0.451	0.464		
	336	0.405	-	0.425	0.430	0.459	0.432	0.440	0.444	0.410	0.426	-	-	0.416	0.418	0.432	0.440	0.413	0.421	0.429	0.416	0.436	0.429	0.428	0.448	0.521	0.492	0.475	0.462	0.451	0.464		
	720	0.448	-	0.470	0.473	0.513	0.482	0.482	0.482	0.479	0.454	0.472	0.523	0.514	0.477	0.456	0.498	0.454	0.447	0.466	0.472	0.490	0.521	0.500	0.506	0.507	0.643	0.616	0.547	0.533	0.608	0.573	
ETTh2	Avg	0.402	-	0.434	0.439	0.476	0.451	0.449	0.450	0.418	0.436	-	-	0.428	0.426	0.440	0.441	0.413	0.431	0.423	0.437	0.457	0.449	0.446	0.467	0.570	0.537	0.491	0.479	0.489	0.491		
	96	0.264	-	0.277	0.327	0.311	0.344	0.303	0.352	0.288	0.345	0.285	0.348	0.285	0.342	0.281	0.300	0.274	0.336	0.289	0.353	0.340	0.358	0.397	0.476	0.458	0.397	0.437	0.327	0.387			
	192	0.321	-	0.340	0.374	0.395	0.391	0.371	0.392	0.348	0.386	-	-	0.354	0.380	0.342	0.351	0.339	0.379	0.383	0.348	0.418	0.404	0.414	0.429	0.439	0.512	0.493	0.520	0.504	0.400	0.435	
	336	0.351	-	0.354	0.384	0.403	0.402	0.371	0.420	0.369	0.408	-	-	0.354	0.380	0.370	0.369	0.352	0.372	0.366	0.363	0.380	0.379	0.379	0.407	0.443	0.453	0.459	0.460	0.466			
ETTh3	Avg	0.327	-	0.344	0.382	0.426	0.428	0.446	0.428	0.449	0.439	-	-	0.405	0.441	0.401	0.381	0.379	0.422	0.603	0.551	0.462	0.468	0.463	0.474	0.562	0.560	0.863	0.672	1.454	0.847		
	96	0.318	-	0.331	0.360	0.332	0.351	0.351	0.349	0.339	0.349	0.384	0.403	0.292	0.346	0.318	0.320	0.290	0.342	0.299	0.343	0.338	0.358	0.375	0.379	0.419	0.386	0.398	0.374	0.400	0.318	0.367	
	192	0.354	-	0.361	0.384	0.403	0.402	0.371	0.420	0.369	0.408	-	-	0.354	0.384	0.371	0.380	0.333	0.374	0.365	0.365	0.384	0.374	0.375	0.379	0.411	0.445	0.459	0.495	0.464	0.438	0.403	0.419
	336	0.376	-	0.391	0.394	0.427	0.420	0.352	0.445	0.352	0.384	-	-	0.366	0.394	0.377	0.384	0.366	0.392	0.369	0.386	0.368	0.410	0.411	0.445	0.449	0.495	0.464	0.438	0.403	0.446		
ETTm1	Avg	0.338	-	0.342	0.388	0.420	0.408	0.501	0.429	0.354	0.391	-	-	0.355	0.395	0.352	0.356	0.330	0.379	0.431	0.447	0.414	0.427	0.437	0.448	0.481	0.456	0.435	0.437	0.381	0.568		
	96	0.169	-	0.195	0.269	0.189	0.257	0.211	0.294	0.243	0.170	0.181	0.269	0.173	0.262	0.159	0.179	0.165	0.255	0.167	0.269	0.187	0.267	0.203	0.257	0.192	0.274	0.206	0.36	0.197	0.271		
	192	0.172	-	0.196	0.270	0.191	0.257	0.211	0.294	0.243	0.170	0.181	0.269	0.173	0.262	0.159	0.179	0.166	0.255	0.167	0.269	0.187	0.267	0.203	0.257	0.193	0.274	0.206	0.36	0.198	0.272		
	336	0.276	-	0.291	0.333	0.467	0.396	0.343	0.377	0.227	0.297	-	-	0.286	0.341	0.271	0.298	0.274	0.329	0.281	0.342	0.321	0.351	0.325	0.36	0.334	0.361	0.442	0.466	0.338	0.366		
ETTm2	Avg	0.338	-	0.346	0.377	0.460	0.445	0.459	0.441	0.275	0.328	0.366	0.388	0.378	0.401	0.352	0.317	0.362	0.385	0.397	0.421	0.408	0.403	0.421	0.417	0.413	0.675	0.587	0.395	0.419	0.446	0.406	
	96	0.172	-	0.195	0.269	0.189	0.257	0.211	0.294	0.243	0.170	0.181	0.269	0.173	0.262	0.159	0.179	0.165	0.255	0.167	0.269	0.187	0.267	0.203	0.257	0.192	0.274	0.206	0.36	0.197	0.271		
	192	0.223	-	0.247	0.270	0.191	0.257	0.211	0.294	0.243	0.170	0.181	0.269	0.173	0.262	0.159	0.179	0.166	0.255	0.167	0.269	0.187	0.267	0.203	0.257	0.193	0.274	0.206	0.36	0.198	0.272		
	336	0.276	-	0.291	0.333	0.467	0.396	0.343	0.377	0.227	0.297	-	-	0.286	0.341	0.271	0.298	0.274	0.329	0.281	0.342	0.321	0.351	0.325	0.36	0.334	0.361	0.442	0.466	0.338	0.366		
ETTm3	Avg	0.264	-	0.272	0.321	0.350	0.353	0.323	0.363	0.256	0.270	-	-	0.266	0.326	0.250	0.257	0.235	0.315	0.324	0.333	0.347	0.309	0.350	0.306	0.409	0.436	0.304	0.347	0.321	0.286		
	96	0.172	-	0.195	0.269	0.189	0.257	0.211	0.294	0.243	0.170	0.181	0.269	0.173	0.262	0.159	0.179	0.165	0.255	0.167	0.269	0.187	0.267	0.203	0.257	0.192	0.274	0.206	0.36	0.197	0.271		
	192	0.223	-	0.247	0.270	0.191	0.257	0.211	0.294	0.243	0.170	0.181	0.269	0.173	0.262	0.159	0.179	0.166	0.255	0.167	0.269	0.187	0.267	0.203	0.257	0.193	0.274	0.206	0.36	0.198	0.272		
	336	0.276	-	0.291	0.333	0.467	0.396	0.343	0.377	0.227	0.297	-	-	0.286	0.341	0.271	0.298	0.274	0.329	0.281	0.342	0.321	0.351	0.325	0.36	0.334	0.361	0.442	0.466	0.338	0.366		
Weather	Avg	0.233	-	0.235	0.263	0.292	0.257	0.369	0.348	0.230	0.281	-	-	0.277	0.327	0.221	0.235	0.227	0.323	0.249	0.360	0.286	0.309	0.360	0.288	0.314	0.261	0.312	0.235	0.286			
	96	0.159	-	0.167	0.203	0.117	0.156	0.188	0.248	0.154	0.209	-	-	0.162	0.212	0.140	0.157	0.149	0.198	0.176	0.237	0.172	0.220	0.237	0.206	0.223	0.182	0.242	0.152	0.210			
	192	0.203	-	0.197	0.248	0.165	0.205	0.265	0.309	0.209	0.214	-	-	0.204	0.248	0.187	0.206	0.194	0.241	0.220	0.282	0.219	0.261	0.276	0.336	0.245	0.285	0.227	0.287	0.199	0.260		
	336	0.247	-	0.232	0.276	0.256	0.278	0.409	0.374	0.248	0.285	-	-	0.258	0.286	0.242	0.255	0.245	0.282	0.263	0.319	0.280	0.306	0.339	0.36	0.321	0.338	0.282	0.344	0.334	0.311		
Weather	Avg	0.233	-	0.235	0.263	0.292	0.257	0.369	0.348	0.230	0.281	-	-	0.237	0.271																		

Table 25: Full results of long sequence forecasting experiments for zero-shot versus fine-tuning. Delphyne-F underperforms both model due to lack of similar dataset in pre-training. Both Delphyne-A and Delphyne-L perform comparatively well after fine-tuning.

Dataset	Delphyne-L-ZS				Delphyne-F-ZS				Delphyne-A-ZS				Delphyne-L-FT		Delphyne-F-FT		Delphyne-A-FT	
	MSE	MAE	MSE	MAE	MSE	MAE	MSE	MAE	MSE	MAE	MSE	MAE	MSE	MAE	MSE	MAE	MSE	MAE
ETTh1	96	0.388	0.418	1.179	0.690	0.398	0.417	0.384±0.001	0.400±0.023	0.403±0.003	0.409±0.011	0.376±0.001	0.390±0.020					
	192	0.437	0.452	1.405	0.769	0.440	0.444	0.445±0.009	0.457±0.010	0.456±0.023	0.493±0.032	0.432±0.011	0.440±0.006					
	336	0.502	0.483	1.677	0.857	0.474	0.464	0.470±0.001	0.490±0.029	0.487±0.040	0.484±0.036	0.452±0.006	0.481±0.035					
	720	0.598	0.526	2.203	1.025	0.482	0.479	0.534±0.013	0.489±0.067	0.517±0.013	0.484±0.042	0.498±0.023	0.454±0.039					
ETTh2	96	0.297	0.354	0.440	0.433	0.303	0.352	0.283±0.005	0.302±0.032	0.328±0.013	0.351±0.045	0.281±0.006	0.300±0.031					
	192	0.368	0.405	0.612	0.513	0.371	0.397	0.352±0.007	0.364±0.014	0.402±0.014	0.393±0.012	0.342±0.001	0.351±0.014					
	336	0.412	0.434	0.799	0.592	0.400	0.420	0.383±0.002	0.389±0.008	0.406±0.017	0.420±0.012	0.382±0.009	0.393±0.007					
	720	0.448	0.462	1.075	0.689	0.428	0.446	0.422±0.015	0.403±0.043	0.433±0.011	0.417±0.028	0.401±0.004	0.381±0.028					
ETTm1	96	0.599	0.455	1.498	0.711	0.439	0.399	0.295±0.004	0.314±0.028	0.313±0.001	0.324±0.014	0.318±0.009	0.320±0.013					
	192	0.715	0.502	1.730	0.780	0.483	0.425	0.348±0.006	0.350±0.007	0.342±0.005	0.350±0.014	0.339±0.005	0.354±0.021					
	336	0.795	0.534	2.006	0.861	0.512	0.445	0.363±0.004	0.382±0.024	0.385±0.014	0.417±0.035	0.377±0.008	0.384±0.016					
	720	0.919	0.581	3.030	1.090	0.572	0.478	0.433±0.014	0.408±0.048	0.482±0.030	0.446±0.069	0.421±0.012	0.402±0.039					
ETTm2	96	0.245	0.313	0.288	0.347	0.211	0.294	0.157±0.002	0.179±0.028	0.159±0.002	0.181±0.029	0.159±0.003	0.179±0.024					
	192	0.351	0.375	0.422	0.418	0.278	0.338	0.221±0.002	0.239±0.024	0.222±0.002	0.246±0.033	0.216±0.002	0.233±0.022					
	336	0.452	0.427	0.583	0.495	0.343	0.377	0.273±0.000	0.305±0.046	0.283±0.007	0.312±0.048	0.271±0.006	0.298±0.035					
	720	0.554	0.480	0.918	0.625	0.459	0.441	0.360±0.007	0.318±0.052	0.373±0.010	0.328±0.059	0.352±0.005	0.317±0.053					
Weather	96	0.197	0.256	0.315	0.295	0.188	0.248	0.141±0.001	0.158±0.026	0.147±0.002	0.165±0.024	0.140±0.002	0.157±0.023					
	192	0.292	0.324	0.416	0.353	0.265	0.309	0.189±0.003	0.207±0.023	0.191±0.002	0.211±0.031	0.187±0.003	0.204±0.026					
	336	0.433	0.390	0.576	0.426	0.409	0.374	0.240±0.002	0.252±0.018	0.246±0.006	0.260±0.025	0.242±0.004	0.255±0.021					
	720	0.633	0.483	1.035	0.576	0.612	0.460	0.311±0.008	0.319±0.012	0.322±0.006	0.332±0.009	0.316±0.008	0.323±0.018					
Electricity	96	0.161	0.259	2.006	1.077	0.164	0.260	0.145±0.002	0.178±0.046	0.164±0.010	0.198±0.041	0.143±0.001	0.176±0.046					
	192	0.180	0.275	2.399	1.160	0.181	0.276	0.159±0.002	0.191±0.047	0.173±0.005	0.205±0.049	0.159±0.002	0.192±0.045					
	336	0.203	0.295	3.151	1.304	0.202	0.296	0.172±0.002	0.204±0.044	0.191±0.003	0.222±0.046	0.173±0.001	0.207±0.047					
	720	0.268	0.342	4.664	1.592	0.260	0.340	0.203±0.003	0.235±0.044	0.233±0.001	0.264±0.044	0.206±0.002	0.238±0.046					

F PROBABILITY QUANTIFICATION

For fine-tuning Delphyne, we use a learning rate of 5e-5, dropout of 0.2, batch size of 128, and a linear warmup for the learning rate of 50 steps. For all datasets, we use a context length of 1000 except Walmart, for which we use 50-100. We use early-stopping based on the validation loss. Similarly, we stick to the default hyperparameters without additional searching.

For evaluation, we use CRPS (Gneiting & Raftery, 2007), MSIS (Makridakis et al., 2020), symmetric mean absolute percentage error (sMAPE) (Hyndman, 2014), mean absolute scaled error (MASE) (Hyndman & Koehler, 2006), normalized deviation (ND), and normalized root mean squared error (NRMSE) (Yu et al., 2016).

The CRPS (Gneiting & Raftery, 2007) is a probabilistic forecasting evaluation metric, given a forecasted distribution with c.d.f. F and ground truth y , it is defined as:

$$\text{CRPS} = \int_0^1 2\Lambda_\alpha(F^{-1}(\alpha), y) d\alpha$$

$$\Lambda_\alpha(q, y) = (\alpha - \mathbf{1}_{y < q})(y - q),$$

where Λ_α is the α -quantile loss, also known as the pinball loss at quantile level α . To compute a normalized metric, the mean weighted sum quantile loss (Park et al., 2022), defined as the average of K quantiles:

$$\text{CRPS} \approx \frac{1}{K} \sum_{k=1}^K \text{wQL}[\alpha_k]$$

$$\text{wQL}[\alpha] = 2 \frac{\sum_t \Lambda_\alpha(\hat{q}_t(\alpha), y_t)}{\sum_t |y_t|},$$

where $\hat{q}_t(\alpha)$ is the forecasted α -quantile at time step t . We take $K = 9, \alpha_1 = 0.1, \alpha_2 = 0.2, \dots, \alpha_9 = 0.9$ in practice.

The MSIS (Makridakis et al., 2020) is a metric to evaluate uncertainty around point forecasts. Given an upper bound forecast U_t (0.975 quantile) and lower bound forecast L_t (0.025 quantile) the MSIS is defined as:

$$\text{MSIS} = \frac{1}{h} \frac{\sum_{t=1}^h (U_t - L_t) + \frac{2}{a} (L_t - Y_t) \mathbb{I}_{\{Y_t < L_t\}} + \frac{2}{a} (Y_t - U_t) \mathbb{I}_{\{Y_t > U_t\}}}{\frac{1}{n-m} \sum_{t=m+1}^n |Y_t - Y_{t-m}|}$$

where $a = 0.05$ is the significance level for a 95% forecast interval, over a forecast horizon of length h , and m is the seasonal factor.

Table 26: Full results for probabilistic forecasting experiments for different Delphyne models. The best results are highlighted in **bold**. Fine-tuning results are averaged across three experimental runs, with reported mean \pm std. Fine-tuning improves the model performances across the board.

		Delphyne-L-ZS	Delphyne-F-ZS	Delphyne-A-ZS	Delphyne-L-FT	Delphyne-F-FT	Delphyne-A-FT
Electricity	CRPS	0.153	0.362	0.159	0.135\pm0.007	0.136 \pm 0.003	0.140 \pm 0.005
	MSIS	30.006	36.197	29.293	27.106 \pm 1.357	24.326 \pm 1.498	21.820\pm1.383
	sMAPE	0.229	0.535	0.233	0.210 \pm 0.008	0.224 \pm 0.007	0.215 \pm 0.008
	MASE	1.972	4.325	2.031	1.783\pm0.089	1.824 \pm 0.039	1.839 \pm 0.080
	ND	0.177	0.453	0.182	0.158\pm0.008	0.163 \pm 0.004	0.164 \pm 0.005
Solar	NRMSE	1.037	2.915	1.084	0.948 \pm 0.034	0.936\pm0.027	0.986 \pm 0.007
	CRPS	0.893	1.126	0.905	1.223 \pm 0.104	1.423 \pm 0.092	1.306 \pm 0.103
	MSIS	2.518	3.279	2.733	1.600\pm0.409	3.085 \pm 0.859	2.029 \pm 0.520
	sMAPE	1.650	1.696	1.650	1.482\pm0.005	1.706 \pm 0.003	1.499 \pm 0.009
	MASE	1.631	1.543	1.710	1.010\pm0.102	2.348 \pm 0.462	1.076 \pm 0.164
Walmart	ND	0.249	0.233	0.263	0.245 \pm 0.016	0.356 \pm 0.070	0.290 \pm 0.028
	NRMSE	2.486	3.070	2.483	1.090 \pm 0.231	4.544 \pm 0.108	1.060\pm0.129
	CRPS	0.096	0.106	0.093	0.091 \pm 0.001	0.103 \pm 0.001	0.083\pm0.001
	MSIS	4.709	5.284	4.741	4.203\pm0.072	4.518 \pm 0.165	4.559 \pm 0.289
	sMAPE	0.185	0.201	0.184	0.079 \pm 0.003	0.193 \pm 0.006	0.088\pm0.003
Weather	MASE	0.666	0.703	0.645	0.669 \pm 0.017	0.719 \pm 0.023	0.660\pm0.002
	ND	0.132	0.142	0.126	0.107 \pm 0.002	0.141 \pm 0.004	0.101\pm0.001
	NRMSE	0.291	0.303	0.270	0.260\pm0.001	0.325 \pm 0.016	0.279 \pm 0.003
	CRPS	0.061	0.074	0.064	0.041\pm0.003	0.045 \pm 0.004	0.042 \pm 0.005
	MSIS	6.012	8.331	6.080	4.600 \pm 0.100	4.304\pm0.092	4.467 \pm 0.053
Istanbul Traffic	sMAPE	0.959	0.812	0.906	0.895 \pm 0.236	1.059 \pm 0.178	0.890\pm0.214
	MASE	0.711	0.834	0.701	0.510 \pm 0.050	0.535 \pm 0.020	0.505\pm0.058
	ND	0.088	0.108	0.095	0.056\pm0.008	0.064 \pm 0.012	0.057 \pm 0.012
	NRMSE	0.255	0.403	0.270	0.209\pm0.007	0.218 \pm 0.016	0.212 \pm 0.015
	CRPS	0.155	0.468	0.149	0.209 \pm 0.007	0.218 \pm 0.016	0.212 \pm 0.015
Turkey Power	MSIS	11.656	15.971	9.989	5.634 \pm 2.351	5.454 \pm 1.433	4.328\pm0.536
	sMAPE	0.724	5.171	0.352	0.236\pm0.018	0.249 \pm 0.021	0.242 \pm 0.017
	MASE	0.799	2.790	0.772	0.580 \pm 0.074	0.611 \pm 0.063	0.558\pm0.018
	ND	0.181	0.632	0.175	0.131 \pm 0.017	0.139 \pm 0.014	0.127\pm0.004
	NRMSE	0.284	0.755	0.273	0.220 \pm 0.031	0.219 \pm 0.025	0.189\pm0.010
	CRPS	0.046	0.148	0.046	0.035 \pm 0.002	0.062 \pm 0.002	0.035\pm0.001
	MSIS	6.299	19.902	6.269	5.462 \pm 0.117	7.856 \pm 0.197	5.384\pm0.346
	sMAPE	0.172	0.277	0.176	0.167\pm0.001	0.195 \pm 0.002	0.168 \pm 0.002
	MASE	0.886	1.753	0.891	0.794 \pm 0.004	1.009 \pm 0.015	0.790\pm0.018
	ND	0.058	0.187	0.059	0.045 \pm 0.002	0.080 \pm 0.002	0.045\pm0.001
	NRMSE	0.132	0.486	0.132	0.096\pm0.006	0.202 \pm 0.010	0.098 \pm 0.003

Table 27: Full results for probabilistic forecasting experiments. The best results are highlighted in **bold**, and the second best results are underlined. (The baseline results are taken from Woo et al. (2024).)

		Zero-shot		Finetuned		Full-shot		Baseline	
		Delphyne-A-ZS	MOIRAI	Delphyne-A-FT	PatchTST	TIDE	TFT	DeepAR	AutoARIMA
Electricity	CRPS	0.159	0.055	0.140 \pm 0.005	0.052 \pm 0.00	0.048\pm0.00	0.050 \pm 0.00	0.065 \pm 0.01	0.327
	MSIS	29.293	6.172	21.820 \pm 1.383	5.744 \pm 0.12	5.672\pm0.08	6.278 \pm 0.24	6.893 \pm 0.82	29.412
	sMAPE	0.233	0.111	0.215 \pm 0.008	0.107 \pm 0.00	0.102\pm0.00	0.106 \pm 0.01	0.118 \pm 0.02	0.318
	MASE	2.031	0.792	1.839 \pm 0.080	0.753 \pm 0.01	0.706 \pm 0.02	0.747 \pm 0.03	0.844 \pm 0.16	3.229
	ND	0.182	0.069	0.164 \pm 0.005	0.065 \pm 0.00	0.061\pm0.00	0.063 \pm 0.00	0.080 \pm 0.02	0.357
Solar	NRMSE	1.084	0.551	0.986 \pm 0.007	0.506 \pm 0.02	0.514 \pm 0.02	0.511 \pm 0.02	0.704 \pm 0.11	3.296
	CRPS	0.905	0.419	1.306 \pm 0.103	0.518 \pm 0.09	0.420\pm0.00	0.446 \pm 0.03	0.431 \pm 0.01	1.055
	MSIS	<u>2.733</u>	7.011	2.029\pm0.520	8.447 \pm 1.59	13.754 \pm 0.32	8.057 \pm 3.51	11.181 \pm 0.67	25.849
	sMAPE	1.650	1.410	1.499 \pm 0.009	1.501 \pm 0.10	1.400 \pm 0.00	1.391 \pm 0.01	1.385\pm0.00	1.685
	MASE	1.710	1.292	1.076\pm0.164	1.607 \pm 0.25	1.265 \pm 0.02	1.399 \pm 0.11	1.222 \pm 0.01	2.583
Walmart	ND	0.263	0.551	0.290 \pm 0.028	0.685 \pm 0.11	0.538 \pm 0.01	0.594 \pm 0.05	0.520 \pm 0.00	1.098
	NRMSE	2.483	1.034	1.060 \pm 0.129	1.408 \pm 0.26	1.093 \pm 0.00	1.236 \pm 0.06	1.033\pm0.01	1.784
	CRPS	0.093	0.093	0.083 \pm 0.001	0.082 \pm 0.01	0.077\pm0.00	0.087 \pm 0.00	0.121 \pm 0.00	0.124
	MSIS	4.741	8.421	4.559\pm0.289	6.005 \pm 0.21	6.258 \pm 0.12	8.718 \pm 0.10	12.502 \pm 0.03	9.888
	sMAPE	0.184	0.168	0.088\pm0.003	0.150 \pm 0.01	0.145 \pm 0.00	0.172 \pm 0.00	0.216 \pm 0.00	0.219
Weather	MASE	0.645	0.964	0.660 \pm 0.002	0.867 \pm 0.09	0.814 \pm 0.01	0.948 \pm 0.02	1.193 \pm 0.02	1.131
	ND	0.126	0.117	0.101 \pm 0.001	0.105 \pm 0.01	0.097\pm0.00	0.108 \pm 0.00	0.147 \pm 0.00	0.141
	NRMSE	0.270	0.291	0.279 \pm 0.003	0.218 \pm 0.02	0.204\pm0.00	0.235 \pm 0.01	0.298 \pm 0.00	0.305
	CRPS	0.064	0.041	0.042 \pm 0.005	0.059 \pm 0.01	0.054 \pm 0.00	0.043 \pm 0.00	0.132 \pm 0.01	0.252
	MSIS	6.080	<u>5.136</u>	4.467\pm0.053	7.759 \pm 0.49	8.095 \pm 1.74	7.791 \pm 0.44	21.651 \pm 17.34	19.805
Istanbul Traffic	sMAPE	0.906	<u>0.623</u>	0.890 \pm 0.214	0.668 \pm 0.01	0.636 \pm 0.01	0.672 \pm 0.01	0.776 \pm 0.05	0.770
	MASE	0.701	0.487	0.505 \pm 0.058	0.844 \pm 0.19	0.832 \pm 0.13	0.692 \pm 0.02	3.170 \pm 3.47	0.938
	ND	0.095	0.048	0.057 \pm 0.012	0.072 \pm 0.02	0.066 \pm 0.01	0.051 \pm 0.00	0.163 \pm 0.15	0.139
	NRMSE	0.270	0.417	0.212 \pm 0.015	0.260 \pm 0.01	0.214 \pm 0.00	0.211 \pm 0.00	0.486 \pm 0.43	0.465
	CRPS	0.149	0.116	0.212 \pm 0.015	0.112 \pm 0.00	0.110 \pm 0.01	0.110 \pm 0.01	0.108\pm0.00	0.589
Turkey Power	MSIS	9.989	4.461	4.328 \pm 0.536	3.813\pm0.09	4.752 \pm 0.17	4.057 \pm 0.44	4.094 \pm 0.31	16.317
	sMAPE	0.352	0.284	0.242\pm0.017	0.287 \pm 0.01	0.280 \pm 0.01	0.287 \pm 0.01	0.249 \pm 0.01	1.141
	MASE	0.772	0.644	0.558\pm0.018	0.653 \pm 0.02	0.618 \pm 0.03	0.620 \pm 0.03	0.613\pm0.03	3.358
	ND	0.175	0.146	0.127\pm0.004	0.148 \pm 0.01	0.140 \pm 0.01	0.141 \pm 0.01	0.139 \pm 0.01	0.257
	NRMSE	0.273	0.194	0.189 \pm 0.010	0.190 \pm 0.01	0.185 \pm 0.01	0.185 \pm 0.01	0.181\pm0.01	0.959
	CRPS	0.046	<u>0.040</u>	0.035\pm0.001	0.054 \pm 0.01	0.046 \pm 0.01	0.039 \pm 0.00	0.066 \pm 0.02	0.116
	MSIS	<u>6.269</u>	6.766	5.384\pm0.346	8.978 \pm 0.51	8.579 \pm 0.52	7.943 \pm 0.31	13.520 \pm 1.17	14.863
	sMAPE	0.176	0.378	0.168 \pm 0.002	0.416 \pm 0.01	0.389 \pm 0.00	0.383 \pm 0.00	0.404 \pm 0.01	0.244
	MASE	0.891	<u>0.888</u>	0.790\pm0.018	1.234 \pm 0.12	0.904 \pm 0.02	0.890 \pm 0.05	1.395 \pm 0.30	1.700
	ND	0.059	0.051	0.045\pm0.001	0.071 \pm 0.01	0.059 \pm 0.01	0.049 \pm 0.00	0.083 \pm 0.02	0.150
	NRMSE	0.132	0.118	0.098\pm0.003	0.158 \pm 0.01	0.139 \pm 0.03	0.104\pm0.01	0.181 \pm 0.05	0.383
	CRPS	0.046	0.040	0.035 \pm 0.001	0.054 \pm 0.01	0.046 \pm 0			

G ANOMALY DETECTION

G.1 ANOMALY DETECTION EXPERIMENT SETUP

Our experimental setup is similar to that of Goswami et al. (2024). Following Goswami et al. (2023), we used a fixed anomaly detection window size of 512 and downsampled all time-series datasets longer than 2560 timesteps by a factor of 10 to speed up the training and evaluation process. We use the mean squared error between forecasts and observations as the anomaly criterion. We get forecasts from our model by masking out nonoverlapping patches of 32 from the window of 512. Even though Delphyne was pre-trained to forecast, we noticed that Delphyne was able to impute values in other parts of each time series. For training, to improve imputation performance, each row of the dataset is to forecast a random patches of size 32, not just at the end of the time series.

G.2 FULL COMPARISON RESULTS

Table 28 shows the full adjusted F_1 results across UCR Anomaly Archive.

Model name	Anomaly Transformer	MOMENT	DGH1	GPT4TS	TimesNet	AnomalyTransformer	Delphyne-A-ZS	Delphyne-A-FT
InternalBleeding4	NaN	NaN	NaN	NaN	NaN	NaN	0.717	0.996
1sddb40	0.030	0.540	0.390	0.190	0.680	0.640	0.818	0.754
BIDMC1	0.990	1.000	1.000	1.000	1.000	0.690	0.390	0.899
CHARISfive	0.010	0.130	0.020	0.020	0.080	0.360	0.017	0.015
CHARISten	0.020	0.110	0.040	0.100	0.030	0.430	0.034	0.040
CIMIS44AirTemperature3	0.060	0.980	0.500	0.180	0.470	0.640	0.167	1.000
CIMIS44AirTemperature5	0.390	0.990	0.960	0.200	0.710	0.780	0.225	1.000
ECG2	1.000	1.000	0.620	0.900	1.000	0.830	0.864	0.772
ECG3	0.360	0.980	0.800	0.840	0.480	0.540	0.142	0.727
Fantasia	0.750	0.950	0.660	0.870	0.550	0.730	0.882	0.833
GP711MarkerLFM5z4	0.930	1.000	0.500	0.640	0.950	0.540	0.837	1.000
GP711MarkerLFM5z5	0.760	0.970	0.310	0.480	0.900	0.690	0.717	1.000
InternalBleeding5	0.940	1.000	1.000	0.920	1.000	0.460	0.883	0.914
Italianpowerdemand	0.010	0.740	0.590	0.010	0.440	0.450	0.087	0.259
Lab2Cmac011215EPG5	0.990	0.980	0.340	0.600	0.990	0.770	0.477	0.672
Lab2Cmac011215EPG6	0.410	0.100	0.260	0.100	0.170	0.700	0.118	0.209
MesoplodonDensirostris	1.000	0.840	0.790	1.000	1.000	0.850	0.532	0.947
PowerDemand1	0.870	0.440	0.490	0.760	0.950	0.720	0.433	0.810
KeepFirstMARS	0.010	0.150	0.020	0.020	0.230	0.520	0.018	0.061
KeepSecondMARS	0.830	1.000	0.160	0.120	0.950	0.720	0.057	0.625
WalkingAcceleration5	0.990	1.000	0.910	0.870	0.930	0.940	0.634	0.843
apneaeeg	0.400	0.200	0.250	0.310	0.260	0.580	1.000	1.000
apneaeeg2	0.650	1.000	1.000	1.000	0.650	0.790	0.213	0.213
gait1	0.180	0.360	0.070	0.410	0.520	0.630	0.204	0.144
gaitHunt1	0.080	0.430	0.020	0.100	0.300	0.810	0.008	0.007
insectEPG2	0.120	0.230	0.140	0.810	0.960	0.650	0.093	0.385
insectEPG4	0.980	1.000	0.460	0.210	0.850	0.690	0.068	0.840
lstdbs30791AS	1.000	1.000	1.000	1.000	1.000	0.780	0.080	0.120
mit14046longtermecg	0.450	0.590	0.530	0.580	0.600	0.790	0.939	0.939
park3m	0.150	0.640	0.200	0.630	0.930	0.630	0.232	0.753
qtdbSel1005V	0.410	0.650	0.400	0.390	0.530	0.520	0.494	0.412
qtdbSel100MLII	0.420	0.840	0.410	0.600	0.870	0.620	0.417	0.402
respiration1	0.000	0.150	0.030	0.010	0.030	0.750	0.006	0.006
s20101mML2	0.690	0.710	0.150	0.050	0.080	0.640	1.000	1.000
sddb49	0.890	1.000	0.880	0.940	1.000	0.660	0.781	0.820
sel840mECG1	0.160	0.660	0.280	0.210	0.360	0.620	0.247	0.235
sel840mECG2	0.150	0.390	0.320	0.280	0.210	0.590	0.484	0.507
tilt12744mtable	0.070	0.240	0.100	0.000	0.030	0.480	0.031	0.080
tilt12754table	0.230	0.640	0.040	0.060	0.050	0.600	0.017	0.084
tiltAPB2	0.920	0.980	0.360	0.830	0.380	0.770	0.416	0.692
tiltAPB3	0.170	0.850	0.030	0.050	0.090	0.680	0.029	0.068
weallwalk	0.000	0.580	0.070	0.130	0.170	0.730	0.041	0.667

Table 28: Anomaly detection performance measured using adj. best F_1 for a subset of 45 datasets sampled from the UCR Anomaly archive.

H NEGATIVE TRANSFER

For all our synthetic data experiments, we train with 8 layers, the attention is of 1024 dimension shared between 8 heads, following to a maximum width of 4098. We used no dropout. The model is trained on negative log likelihood loss of a Gaussian. The model was trained on 100K steps with a fixed patch size of 1. For optimization, we used a batch size of 64 and employed the AdamW optimizer with the following hyperparameters: $lr = 1e-4$, weight decay = $1e-5$, $\beta_1 = 0.9$, and $\beta_2 = 0.98$. A learning rate scheduler was applied, featuring linear warmup for the first 5,000 steps, followed by cosine annealing down to $1e-5$.

For our synthetic data, we use wavelet functions:

$$\begin{aligned} x_t &= (d * t/T - c) \sin(a * t + b) + \epsilon_t \\ \epsilon_t &\sim \mathcal{N}(0, 0.2) \end{aligned}$$

where the parameters are $\{a, b, c, d\}$ and T is the number of time steps of the time series, and GARCH:

$$\begin{aligned} x_t &= \mu + \epsilon_t \\ \epsilon_t &\sim \mathcal{N}(0, \sigma_t) \\ \sigma_t^2 &= \omega + a x_{t-1}^2 + b \epsilon_{t-1}^2 \end{aligned}$$

where the parameters are $\{\omega, a, b, \sigma_0, \mu\}$.

H.1 PRE-TRAINING WITH GARCH AND WAVELET DATA

For generating GARCH data, we use:

$$\begin{aligned} \mu &= 0 \\ \sigma_0 &= \omega \sim U(0, 1) \\ a &\sim U(0, 1) \\ b &\sim U(0, 1 - a) \end{aligned}$$

For generating wavelet data, we use:

$$\begin{aligned} a &\sim \{0.1, 0.2, 0.6, 0.8\} \\ b &\sim \{0, 5, 10\} \\ c &\sim \{0.0, 0.3, 0.6, 0.9\} \\ d &\sim \{0.5, 0.9\} \end{aligned}$$

where the sets denote a uniform sample from those choices.

H.2 BAYESIAN MCMC

For the wavelet distribution, we use:

$$\begin{aligned} T &= 32 \\ a &\sim U(0, 1) \\ b &\sim U(0, 1) \\ c &\sim U(0, 1) \\ d &\sim U(0, 1) \end{aligned}$$

where U denotes a Uniform distribution.

For the GARCH distribution, we use:

$$\begin{aligned} \mu &= 0 \\ \sigma_0 &= \omega = 0.3^2 \\ a &\sim U(0, 0.2) \\ b &\sim U(0, 0.2) \end{aligned}$$

For computing the NLL and the mean, we need to find the probability that a time-series comes from each distribution. For this, we computed the log-likelihood through 10K samples from the prior. For computing the posterior of the parameters given the data for each model, we use the NUTS sampler (Hoffman & Gelman, 2014).

I ADDITIONAL ABLATION STUDIES

For pre-training, we use the same setup as in Section H. For fine-tuning, similar to fine-tuning Delphyne, we early-stop based on a validation set.

I.1 CONTEXT LENGTH

For these experiments, we use the same wavelet data generation as in Section H.1. We used a finite set of configurations to test how well the model is able to create features specific to a dataset. The intuition is that with a smaller context length, the pre-training does not create features specific to the type of wavelet that generated the data but longer context lengths do.

I.1.1 ARCHITECTURE FOR CONTEXT LENGTHS

Small The small model is a transformer encoder of 6 encoder layers, a context length of 128, and a hidden dimension size of 512. It uses 8 attention heads, a feedforward dimension of 2048, and applies a GELU activation function. The model is designed to output attention weights, and features a dropout rate of 0.1 to prevent overfitting. It is trained using the Adam optimizer with a learning rate of 1e-4, betas of 0.9 and 0.98, and a weight decay of 1e-5. The configuration includes training, validation, and test batch sizes of 128, with warmup steps for the learning rate set at 5,000 out of 100,000 total training steps.

Medium The medium model contains 8 encoder layers and a context length of 128, featuring a hidden dimension size of 1024. The model uses 8 attention heads and a feedforward dimension of 4096 with GELU activation, while a dropout rate of 0.1 is applied for regularization. The model outputs attention weights and employs batch sizes of 64 for training, validation, and testing. It uses the Adam optimizer with a learning rate of 1e-4, betas of 0.9 and 0.98, a weight decay of 1e-5, and includes 5,000 warmup steps in a total of 100,000 training steps.

I.2 MASKING RATIO

For these experiments, we use the same wavelet data generation as in Section H.1.

I.3 MULTIVARIATE

For these experiments, we use the same wavelet data generation as in Section H.1. The main difference is each sample is four time series. We model two scenarios: one where the Wavelet data across rows are correlated, and another where they are uncorrelated. In the correlated scenario, the time-series data is generated using the same Wavelet function, differing only by additive Gaussian noise. In the uncorrelated scenario, the data is generated using different Wavelet functions.

I.4 OUTPUT DISTRIBUTION

We use the same hyperparameter configuration for training Delphyne-A, on three different output distributions: (1) Single Student T, (2) a mixture of Student-T distributions, and (3) a mixture of Normal, Student’s-T, Log-normal, and negative binomial distributions. For every 10,000 training steps, we finetune the models on stock NLL task in the experiment section. The overall results are shown in Fig. 4.

J LIST OF POPULAR MODELS

We provide a full table of the foundation models in Table 29. We compare popular models between 2022-2024: MOMENT (Goswami et al., 2024), MOIRAI (Wang et al., 2024a), Lag-Llama (Rasul et al., 2023), Chronos (Ansari et al., 2024), TimesFM (Das et al., 2024), TimeGPT-1 (Garza & Mergenthaler-Canseco, 2023), TTM (Ekambaram et al., 2024).

Among these popular models, only MOIRAI, Lag-Llama and TimeGPT-1 are able to provide output distributions and uncertainty quantifications. Specifically, Lag-Llama utilizes a single Student’s T distribution which is less ideal to model asymmetries in forecasts, which is shown in our previous experiment. TimeGPT-1 uses a categorical output distribution. While it may potentially model any multi-modal distributions, the output distribution is tied to TimeGPT-1’s language model architecture and training objective, offering less flexibility overall. Delphyne utilizes a mixture of Student’s T distributions, which are simpler and more stable, as shown in our previous study.

Table 29: Comparison of Pre-trained Time-series Model

Feature	MOMENT (Goswami et al., 2024)	MOIRAI (Woo et al., 2024)	Lag-Llama (Rasul et al., 2023)	Chronos (Ansari et al., 2024)	TimesFM (Das et al., 2024)	TimeGPT-1 (Garza & Mergenthaler-Canseco, 2023)	TTM (Ekambaram et al., 2024)	Delphyne (This paper)
Base Architecture	T5 encoder	Encoder-only	Llama	T5 (encoder-decoder)	Decoder-only	Transformer	MLP-Mixer	Encoder-only transformer
Evaluation Tasks	Forecasting, Classification, Anomaly detection, Imputation	Forecasting	Forecasting	Forecasting	Forecasting	Forecasting	Forecasting	Forecasting, Anomaly detection
Tokenization	Fixed-length patches	Multi-scale Patches	Lag features	Scaling, Quantization	Fixed-length patches	?	Adaptive Patching	Fixed-length patches
Objective	Reconstruction Error	Forecast NLL of mixed-distributions	NLL of Student's t distribution	Cross-entropy loss	Forecast Error	?	Forecasting Error	Forecast NLL of mixture of Student T's distributions
Distribution Prediction / Uncertainty Quantification	✓	✓	✓		✓ (post hoc)		✓	
Multivariates?	✓ (Anyvariate attention w. Channel independence)	✓ (Anyvariate attention + Flattening)		✓		✓ (?)	(Channel Independence + Mixing)	✓ (Anyvariate attention + Flattening)
Context length	512	1000-5000	1024	512	512	?	512	512 x 32

Many existing time-series foundation models excel in modeling single variates, which ignore the potential dependencies between variates (for example, when modeling US stock returns, many stocks in the same sectors are inter-correlated). We use the same any-variate attention mechanism as MOIRAI; we demonstrate in the previous section that any-variate attention performs reasonably well when both the variates are strongly or weakly correlated.

While many pre-trained time-series model aim to adapt to different forecast lengths, TTM has fixed forecast lengths. Its public model has a maximum context length of 1024 and a forecast length of 96, which is limited for various financial tasks. We argue that a good pre-trained time-series model should be agnostic to downstream tasks' forecast lengths and number of variates. In this context, Delphyne offers more flexibility.

Many popular time-series models, such as MOIRAI, Lag-Llama, and TTM, employ various patch sizes or use additional frequency information to capture different frequencies within datasets. We argue that these different patching methods aim to address the negative transfer effect across datasets. Since datasets across domains are collected at varying frequencies, these models leverage frequency information to create distinct embeddings for data at different granularities. In contrast, we believe that fine-tuning, despite being a post-hoc solution, offers the most effective means of mitigating the negative transfer effect.

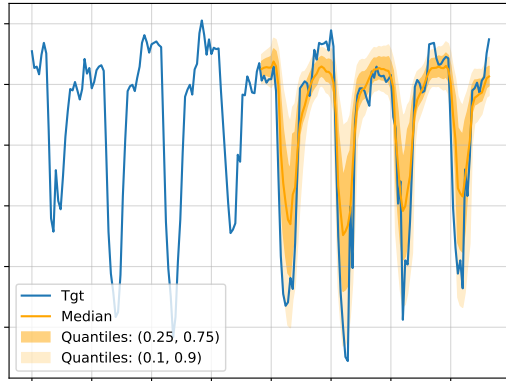


Figure 8: Visualization of fine-tuned forecasts from Delphyne-A on ETTh1 dataset. The quantiles represented are 0.1, 0.25, 0.5, 0.75, and 0.9.

K VISUALIZATIONS

Fig. 8 shows the visualization on ETTh1. Fig. 9 and Fig. 10 show the fine-tuned forecast visualizations on stock variance and NLL. Fig. 11 shows the forecast of nowcasting company revenue. Fig. 12, Fig. 13 and Fig. 14 show the forecast on bars data using Delphyne, MOMENT and TTM.

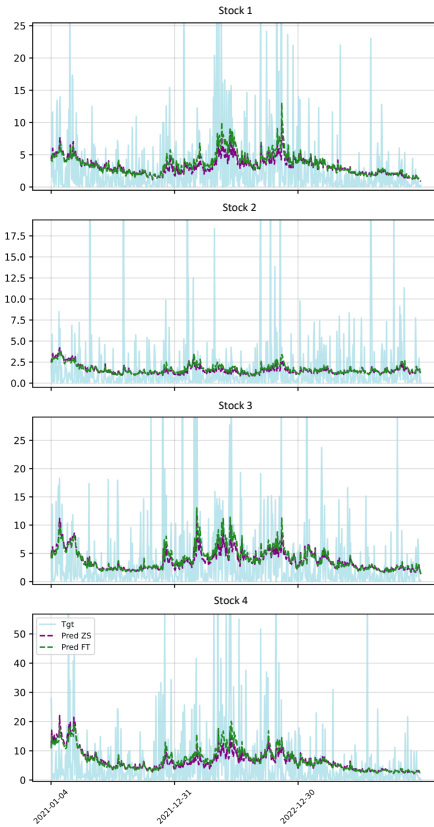


Figure 9: Visualization of fine-tuned forecasts from Delphyne-A on Stock Variance dataset. Note that since sometimes the squared returns are very large, we clip the plot but not the data during training and evaluation.

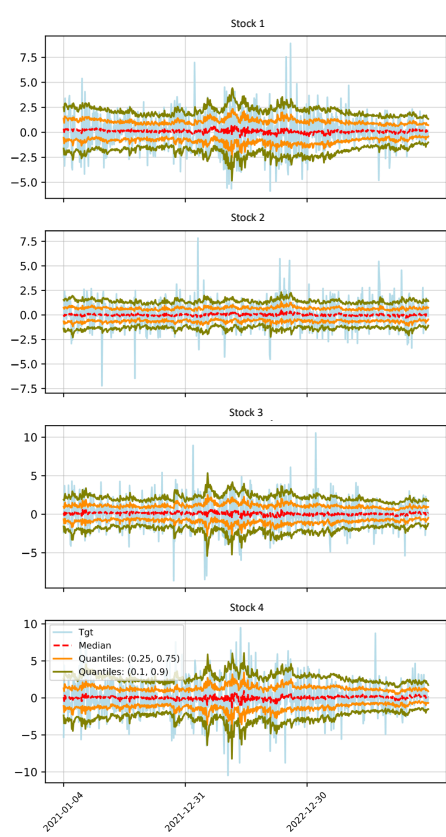


Figure 10: Visualization of fine-tuned probabilistic forecasts from Delphyne-A on Stock NLL dataset.

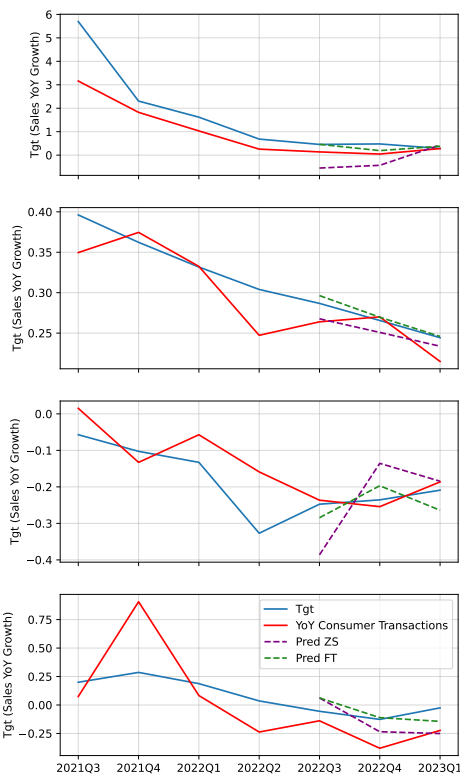


Figure 11: Visualization of fine-tuned forecasts from Delphyne-A on Nowcasting Company Revenue dataset.

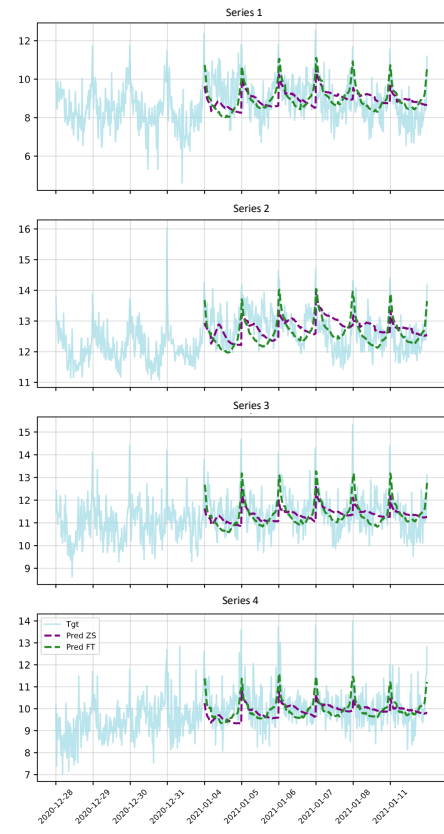


Figure 12: Visualization of fine-tuned forecasts from Delphyne-A on Financial Bars dataset.

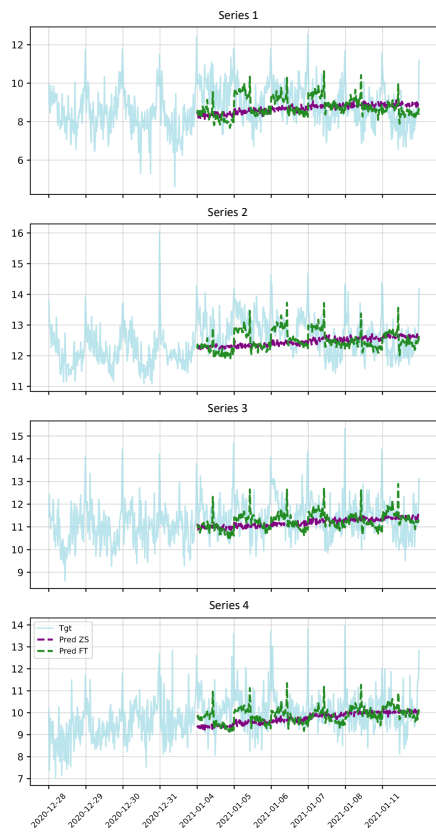


Figure 13: Visualization of fine-tuned forecasts from MOMENT on Financial Bars dataset.

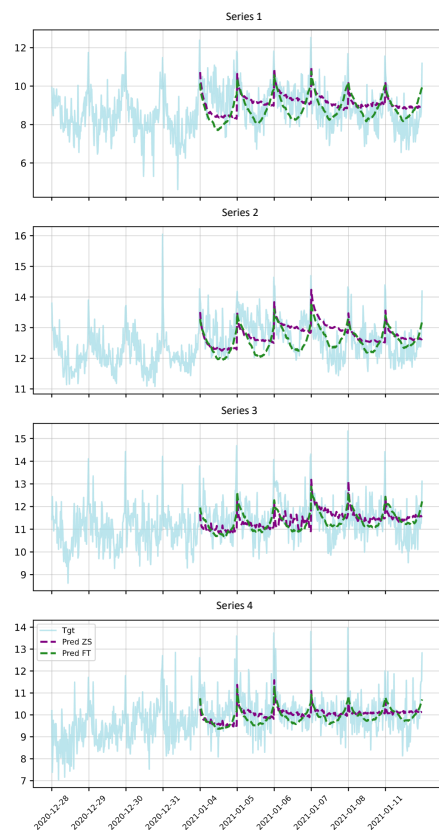


Figure 14: Visualization of fine-tuned forecasts from TTM on Financial Bars dataset.